A MATERIALS VIEW OF ICE

by

ERLAND M. SCHULSON

THAYER SCHOOL OF ENGINEERING

AN ASSOCIATED SCHOOL OF DARTMOUTH COLLEGE, HANOVER, NEW HAMPSHIRE

A MATERIALS VIEW OF ICE

by

ERLAND M. SCHULSON

Thayer School of Engineering
Dartmouth College
Hanover, N.H. 03755

July 15, 1982

(revised December 17, 1982)

Prepared for

SHELL DEVELOPMENT COMPANY
Houston, Texas

ABSTRACT

This report considers the mechanical properties of ice Ih from a materials point of view. Topics include physically based constitutive relationships, uniting strain rate, stress and temperature; strength under uniaxial tension and compression; the effects on strength of grain size, specimen size and surface condition (?); the effect on the compressive peak stress of hydrostatic pressure and of general multiaxial loading in compression; and the role of fracture mechanics in predicting the strength of ice containing flaws. A number of explanations are presented, and a "working hypothesis" is proposed for predicting the peak strength of a multiaxially loaded columnar ice. Four appendices are included: the first presents an experimental sub-study on the velocity of ultrasonic waves through sea ice; the second is a comment on a criticism of the Arrhenius description of the thermal dependence of creep; the third considers an analytical basis for incorporating pressure-melting effects into the constitutive relationships for ice; and the fourth considers grain growth in ice at -10°C.

TABLE OF CONTENTS

SUMMARY

This report considers ice from a materials perspective, with the goal of obtaining insight into the mechanical behavior of an ice sheet as it moves against an engineered structure. The main pointsare summarized as follows:

(i) The relationships between the rate at which ice deforms plastically and the stress driving that deformation are presented mathematically in terms of the physical parameters characteristic of ice, and graphically in terms of deformation mechanism maps as published in the literature. The latter is particularly useful, because it indicates the range of temperature and stress (or deformation rate) over which empirical relationships are expected to be valid. Moreover, it provides quantitative data for any point in temperature/stress space for steady-state flow. Deformation rates under complex states of loading are incorporated in terms of the shear stress effective in promoting plastic flow. One shortcoming, which could be overcome with additional analysis, is that neither the mathematical formulations nor the maps as now developed consider short-term (i.e. transient) behavior.

(ii) The load-bearing capacity of ice under tension is generally determined by the stress required to nucleate cracks, in which case the strength increases as grain size decreases. If cracks exist prior to loading, then the tensile strength is probably controlled by the length of the crack and by the inherent resistance of the material to crack propagation (i.e. by its fracture toughness).

(iii) When slowly strained, the load-bearing capacity of ice under compression (the so-called peak strength) appears to be controlled by a combination of localized cracking and plastic deformation. Hydrostatic pressure suppresses cracking, and thereby allows the peak strength to increase significantly and "ductile" behavior to be observed at relatively high ($\gtrsim 10^{-3}$ sec^{-1}) rates of straining. Whether grain size affects the peak compressive strength remains to be studied carefully.

(iv) Under multiaxial loading, the peak strength of sheets of columnar-grained (S2) saline ice increases dramatically. For example, at -10°C and at moderate rates of straining, the peak strength increases by approximately five times under symmetrical biaxial loading in the plane of the sheet and by more than eight-fold under symmetrical in-plane loading plus loading perpendicular to the plane of the sheet. An analysis of published data suggests that if the ratio of the three principal stresses is known, then the peak strength can be predicted by invoking the concept of a critical shear stress.

(v) Comparison with ceramics suggests that while the tensile strength of ice may be sensitive to its surface condition, annealing following surface preparation is an effective method for reducing such sensitivity. An analysis based upon surface diffusion predicts reasonably well the time and temperature needed to suppress surface sensitivity in ground ceramics, and suggests that a one-day anneal at -10°C should be sufficient to suppress sensitivity in coarse-grained ice.

(vi) The nucleation and propagation of cracks play a major role in determining the strength of ice. Cracks, once nucleated by slip, may grow slowly, may increase in number, or may propagate rapidly if the tensile stress normal to the plane in which they lie is sufficiently large. The resistance to cracking is thus of major interest when dealing with ice forces on structures. Under tensile loading or bending, upper and lower limits on ice strength, respectively, can be estimated from the stress to nucleate cracks within an aggregate of a given grain size and from the stress to propagate pre-existing cracks. The upper limit is calculated from dislocation micromechanics and the lower limit, from fracture mechanics.

(vii) Experiments performed during the course of this study revealed that the velocity of sound waves through ice taken from pressure ridges within the Beaufort Sea appears to be independent of the depth beneath the surface from which the ice was taken. In view of the variability of the ice examined, it is probable that the velocity of sound through ice, unlike that through cast iron, will not correlate with the tensile strength of this material.

A MATERIALS VIEW OF ICE

ERLAND M. SCHULSON
Thayer School of Engineering
Dartmouth College
Hanover, N.H. 03755

July 15, 1982
(revised December 17, 1982)

I. INTRODUCTION

The purpose of this report is to present the results of some part-time thinking over the past six months on the subject of ice Ih as a material. Mechanical behavior was of foremost concern and so the report is restricted to this aspect of the subject. Many of the explanations and analyses are tentative and require further testing through experiment. They are included because they may help to guide experiment and, possibly, to interpret results.

During the course of the work, a question arose concerning the possibility of using ultrasonics, particularly wave velocity, to characterize sea ice. This method is currently being used to characterize cast iron[1] and provides a means for predicting the tensile strength of that material. A small experimental program was thus carried out. The results were reported earlier[2] but, for completion, are given in Appendix 1 as a separate report, entitled: "The Velocity of Ultrasonic Waves Through Sea Ice Taken from Pressure Ridges Within the Beaufort Sea".

We open with a short consideration of the effect of porosity on Young's Modulus, another point which arose during the course of the work.

2. YOUNG'S MODULUS AND POROSITY

The elastic moduli of solids are measures of the variations in spacing of the individual atoms when the solid is stressed. These moduli, therefore, are directly related to the energy which binds the solid together or, more

specifically, to the curvature of the inner potential function at the equilibrium atomic spacing. Defects such as impurity atoms, dislocations and grain boundaries comprise only a small portion of the total number of atoms within a solid and so modify only a small fraction of the atomic bonds. For this reason, the elastic moduli are essentially insensitive to the microstructural features noted. They are, however, sensitive to second phases. In ice, this translates to a sensitivity to brine pockets and to air bubbles; i.e. to porosity.

Appropriate functions to account for the effect of porosity, p, on Young's Modulus, E, were obtained from the ceramics literature which contains information on the effect of porosity (which remains after sintering powders together) on mechanical properties. One of the functions employed is:[3]

$$E = E_0 \left(\frac{1 - p}{1 + Ap} \right) \qquad (1)$$

where A is a numerical constant. Another, derived specifically for spherical holes and for a solid whose Poisson's ratio $\simeq 0.3$, is:[4]

$$E = E_0 (1 - 1.9p + 0.9 p^2). \qquad (2)$$

Note that both expressions reduce to $E = E_0$ and to $E = 0$ in the limits $p = 0$ and $p = 1$, respectively. E_0 is the modulus of ice of theoretical density.

Equation (2) has been applied to sintered alumina[5] with excellent agreement. For this reason and because Poisson's ratio for ice is $\simeq 0.3$, it is the one suggested for ice. Figure 1 shows the variation in E/E_0 which is to be expected on this basis. Note that a porosity of 10% imparts > 10% reduction in E.

The above equations apply strictly for pores of one size distributed more or less uniformly throughout the material. Variations in size, in distribution and in shape may affect the relationship.

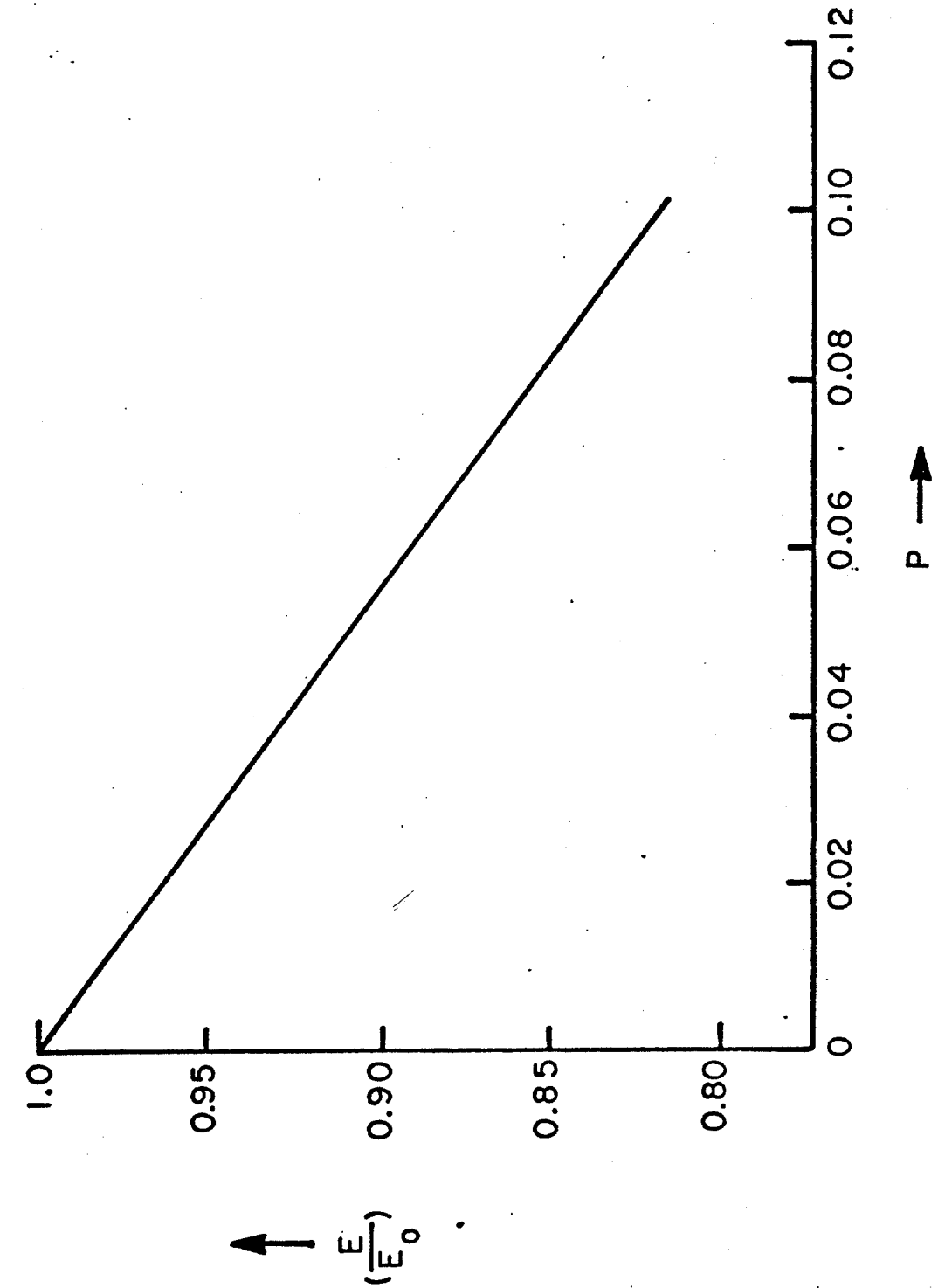

Figure 1. Graph indicating the effect of porosity, p, on the Young's Modulus, E, of a porous material relative to the modulus, E_0, of a non-porous material

3. CONSTITUTIVE EQUATIONS AND DEFORMATION MECHANISM MAPS

In dealing with the plasticity of materials, it is desirable to have available a series of constitutive relationships which connect stress, strain rate and temperature. Preferably, such relationships should be based upon the mechanisms underlying plastic flow and, accordingly, should include materials parameters such as shear modulus, diffusion coefficients, grain size, dislocation density, etc. Physically based relationships are more desirable than empirical ones, because they delineate regions in temperature - stress space within which particular relationships between stress and strain rate are valid. In other words, they indicate just how far one particular relationship can be extrapolated meaningfully.

Ideally, constitutive relationships should also incorporate strain and time induced changes in the microstructural state of the material -- i.e. transient flow as well as steady-state behavior should be included. However, such "all encompassing" relationships based entirely upon physics have not yet been developed, mainly because the microstructural state during transient flow is not well understood in any material.

Attention here is thus focused on the steady-state behavior of equiaxed and randomly oriented polycrystals. The goal is to consider the physically based constitutive laws for ice, and to present these laws graphically in the form of a deformation mechanism map. While isotropic ice is featured, extension of the idea to textured (e.g. S2) ice could be made through geometrical factors, derived and verified by creep experiments, which relate the orientation of the slip planes to the axes of loading.

What are the underlying mechanisms? Which one dominates under a specific set of conditions? Concerning the first question, there are relatively few processes which lead to plastic flow, not only in ice, but also in other crystalline solids. These are:

- Dislocation glide or slip, which is controlled by the atomic bonding, by crystal structure, and by obstacles such as grain boundaries and other dislocations.

- Dislocation glide plus climb, leading to power law creep (termed Glen's Law in the ice literature) known also as dislocation creep.
- Diffusional flow in which atomic diffusion occurs either through the lattice (termed Nabarro-Herring creep) or along the boundaries of grains (termed Coble creep).

Generally, dislocation glide dominates the deformation process at temperatures below $\simeq 0.3\ T_m$, where T_m is the absolute melting temperature; i.e. at temperatures where thermal energy is insufficient to activate the movement of vacancies. This mechanism may also dominate at much higher temperatures under high rates of deformation ($\simeq 10^{-1}$ sec^{-1}). Dislocation creep becomes important at temperatures above about $0.3\ T_m$, where dislocations not only glide under applied shear stresses but also climb via the migration of a vacancy to the core of edge dislocations. Plastic flow is thus possible at a lower stress than would be required for glide only. Diffusional flow operates at high temperatures and at stresses which are too low to move dislocations at significant speeds. In this mechanism, atoms diffuse from specific sources on grain boundaries which bear a compressive stress to sinks on other grain boundaries which bear a tensile stress. Diffusion from source to sink, which occurs across the grain by lattice diffusion, is termed Herring-Nabarro creep, while diffusion along grain boundaries is called Coble creep.

Mathematical expressions have been developed for each of these processes, based upon physical parameters. Generally they express the steady-state strain rate as a function of temperature and shear stress; grain size and dislocation density are included where appropriate. Models applicable to a variety of ionically, covalently and metallically bonded solids can be found in reference (6) where the first deformation map for ice appears.

Concerning ice, theory[7] indicates that only two of the above mechanisms are important -- dislocation glide and diffusional flow. Dislocation creep,

in which the rate-limiting step is the diffusion of vacancies to edge dislocations (climb being slower than glide), appears not to be significant here, evident from the facts that additions of HF ($\lesssim$ few ppm) increase[8] the creep rate but have no effect[9] on the diffusion rate of tritium which diffuses in ice at the same rate as H_2O.[10] Glide and diffusional deformation have been modelled[7] and the formulations are listed in Table 1. Note that the expression given for glide which dominates at high stresses incorporates an exponential term* which decreases in magnitude with increasing stress, implying that the thermal sensitivity of the strain (or creep) rate decreases with increasing stress. The meaning of the symbols and their values are listed in Table 2.[7]

Given the constitutive relations, one can calculate the strain rate produced by each mechanism for a given set of experimental or field conditions. Since glide and diffusional flow are independent processes, the total (steady-state) strain accumulated is the sum of that produced by each mechanism acting separately, in which case the total (steady-state) strain rate, $\dot{\gamma}$, is also the sum of the two individual rates; i.e.

$$\dot{\gamma}_T = \dot{\gamma}_{glide} + \dot{\gamma}_{diffusion}.$$

The dominant mechanism is the one which contributes more than the other for a given set of conditions.

This kind of analysis can be expressed as a plot in temperature - stress space, one plot for a given grain size. In so doing, one obtains a visual impression which shows the region over which one mechanism dominates. Boundaries -- i.e. where two mechanisms contribute equally -- are defined by equating pairs of constitutive equations and then by solving for stress as a function of temperature. Graphical presentations of this form are termed deformation mechanism maps.[11] Any pair of values for temperature and stress locates a point on the map which then identifies the dominant mechanism (or mechanisms if the point falls on a boundary). The strain rate can then be

*Comments on the Arrhenius description of deformation rate are given in Appendix 2.

Table 1. Formulation of constitutive relations for equiaxed and randomly oriented polycrystalline ice[7]*

Mechanism	Controlling Process	Stress Regime	Basis for Model	Constitutive Relationship
Dislocation Glide	Proton rearrangement	Low	Physical	$\dot{\gamma}_{\text{low stress}} = a_0 \left(\frac{\sigma_s}{G}\right)^3 \frac{Gb^3}{kT} \upsilon_o \exp\left(-(E_f + E_m + E_k)/kT\right)$
Dislocation Glide	Proton rearrangement and Kink nucleation on dislocations	High	Physical	$\dot{\gamma}_{\text{high stress}} = \dot{\gamma}_{LS} \left(\frac{kT}{2.5\ \sigma_s\ b^3}\right)^{\frac{1}{2}} \left(1 - \frac{\sigma_s}{G} 4\pi\right)^{-\frac{1}{2}} \times \exp\left(\frac{E_k}{kT}\left(\frac{\sigma_s}{\sigma_o}\right)^{\frac{1}{2}} - 0.06\left(\frac{G}{\sigma_s}\right)^{\frac{1}{2}}\right)$
Diffusional Flow		Low	Physical	$\dot{\gamma}_s = \frac{42\ \sigma_s\ \Omega D_l}{kTd^2} \left(1 + \pi \frac{\delta}{d} \frac{D_b}{D_v}\right)$

*The parameters are defined and their values given in Table 2.

Comments on a recent criticism[35] concerning the appropriateness of the exponential description of deformation rates are made in Appendix 2.

Table 2. Data used by Goodman, Ashby and Frost (ref. 7) for constructing deformation mechanism maps

Atomic volume	Ω	3.27×10^{-29} m^3
Burgers vector	b	4.52×10^{-10} m
Melting temperature	T_m	273·15 K
Shear modulus (adjusted to 300 K)	G	2.91 GN m^{-2}
Temperature dependence of the modulus	(1/G)(dG/dT)	1.29×10^{-3} K^{-1}
Pre-exponential for lattice diffusion	D_{ov}	9.13×10^{-4} m^2 S^{-1}
Lattice diffusion coefficient	$D_l = D_{ov} e^{-Q_l/kT}$	
Activation energy for lattice diffusion	Q_l	59.4 kJ mol^{-1}
Pre-exponential for boundary diffusion	D_{ob}	9.13×10^{-4} m^2 S^{-1}
Grain boundary diffusion coefficient	$D_b = D_{ob} e^{-Q_b/kT}$	
Activation energy for boundary diffusion	Q_b	38.3 kJ mol^{-1}
Width of boundary diffusion path	δ	9.04×10^{-10} m
Pre-exponential for proton-rearrangement controlled glide	a_o	1.2×10^3
Activation energy for proton-rearrangement controlled glide	$E_{PR} = (E_f + E_m + E_k)$	78.1 kJ mol^{-1}
Mean time between proton rearrangements at 0 K	$1/\nu_0$	6.36×10^{-16} S
Stress constant in equation for proton-rearrangement controlled glide	σ_0/G	0.015
Ideal shear strength (normalized)	σ_{th}/G	0.10
Defect creation stress (Glen stress)	σ_G/G	0.10
Energy to form Bjerrum defect	E_f	$E_f + E_m$ = 54.2 kJ mol
Energy to move Bjerrum defect	E_m	
Energy of a kink	E_k	23.9 kJ mol^{-1}
Boltzmann's constant	k	1.38×10^{-23} J/K
Grain diameter	d	

Table 2. Data used by Goodman, Ashby and Frost (ref. 7) for constructing deformation mechanism maps

Atomic volume	Ω	3.27×10^{-29} m^3
Burgers vector	b	4.52×10^{-10} m
Melting temperature	T_m	273·15 K
Shear modulus (adjusted to 300 K)	G	2.91 GN m^{-2}
Temperature dependence of the modulus	(1/G)(dG/dT)	1.29×10^{-3} K^{-1}
Pre-exponential for lattice diffusion	D_{ov}	9.13×10^{-4} m^2 S^{-1}
Lattice diffusion coefficient	$D_l = D_{ov} e^{-Q_l/kT}$	
Activation energy for lattice diffusion	Q_l	59.4 kJ mol^{-1}
Pre-exponential for boundary diffusion	D_{ob}	9.13×10^{-4} m^2 S^{-1}
Grain boundary diffusion coefficient	$D_b = D_{ob} e^{-Q_b/kT}$	
Activation energy for boundary diffusion	Q_b	38.3 kJ mol^{-1}
Width of boundary diffusion path	δ	9.04×10^{-10} m
Pre-exponential for proton-rearrangement controlled glide	a_o	1.2×10^3
Activation energy for proton-rearrangement controlled glide	$E_{PR} = (E_f + E_m + E_k)$	78.1 kJ mol^{-1}
Mean time between proton rearrangements at 0 K	$1/\nu_0$	6.36×10^{-16} S
Stress constant in equation for proton-rearrangement controlled glide	σ_0/G	0.015
Ideal shear strength (normalized)	σ_{th}/G	0.10
Defect creation stress (Glen stress)	σ_G/G	0.10
Energy to form Bjerrum defect	E_f	$E_f + E_m$ = 54.2 kJ mol
Energy to move Bjerrum defect	E_m	
Energy of a kink	E_k	23.9 kJ mol^{-1}
Boltzmann's constant	k	1.38×10^{-23} J/K
Grain diameter	d	

calculated from the appropriate constitutive relation. Deformation mechanism maps are useful because they identify the constitutive law or the combination of laws which should be used in engineering design.

Maps can be modified to include contours of constant strain rate. This is achieved by setting the strain rate to a constant value and then by solving for temperature as a function of stress as dictated by the constitutive relationship for the dominant mechanism. A point on a modified map then indicates not only the dominant strain-producing mechanism, but also the rate of deformation. Modified maps for metals and ceramics are now available in the form of a compendium.[12] They are useful because they allow an immediate estimate of the strain rate of a material or component under stress, at least under conditions of steady state.

Returning to ice, Figures 2, 3 and 4 show three modified maps for ice of three different grain sizes (0.1 mm, 1 mm and 10 mm). They indicate, for instance, that non-textured aggregates of 1 mm grain size flow at 10^{-4} sec^{-1} at -10°C under an effective shear stress of 3 MPa. Note that grain refinement expands the diffusional field at the expense of the glide field, and that it moves to higher temperatures the boundary between Herring-Nabarro and Coble creep (i.e. volume vs. boundary diffusional creep). The maps are plotted in terms of equivalent or effective shear stress, and so can be used to estimate strain rates under conditions of multiaxial loading; the equivalent shear stress is given as:

$$\sigma_s = \frac{1}{\sqrt{3}} \left\{ \frac{1}{2} \left[(\sigma_1-\sigma_2)^2 + (\sigma_2-\sigma_3)^2 + (\sigma_3-\sigma_1)^2 \right] \right\}^{\frac{1}{2}} \qquad (3)$$

where σ_1, σ_2 and σ_3 are the principal stresses. Similarly, the contours are of equivalent shear strain rate given by

$$\dot{\gamma} = \left\{ \frac{2}{3} \left[(\dot{\varepsilon}_1 - \dot{\varepsilon}_2)^2 + (\dot{\varepsilon}_2 - \dot{\varepsilon}_3)^2 + (\dot{\varepsilon}_3 - \dot{\varepsilon}_1)^2 \right] \right\}^{\frac{1}{2}} \qquad (4)$$

where $\dot{\varepsilon}_1$, $\dot{\varepsilon}_2$ and $\dot{\varepsilon}_3$ are the principal strain rates.

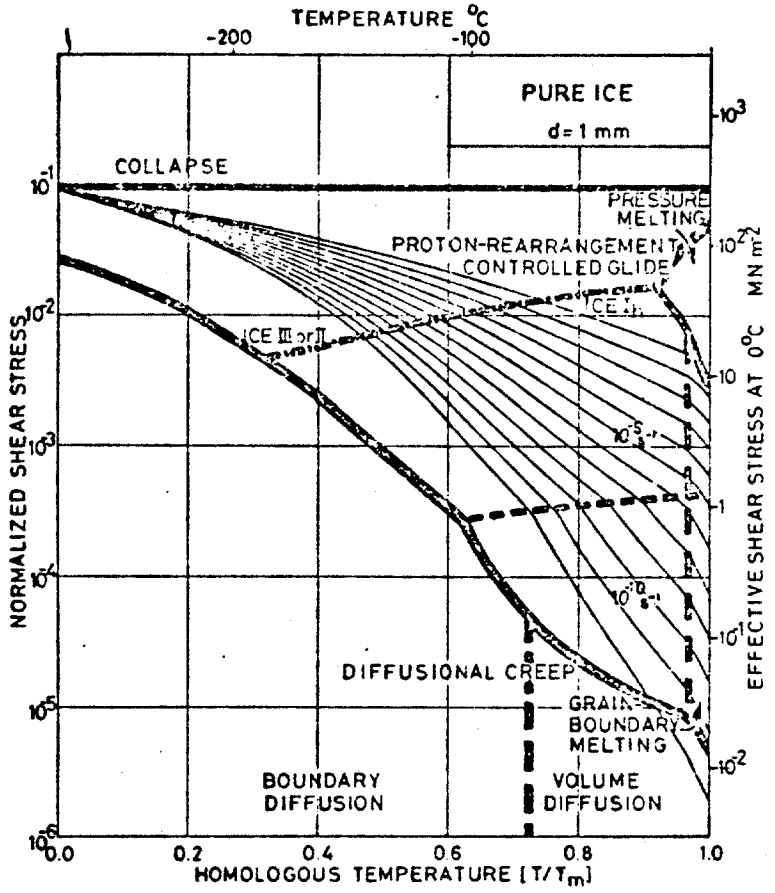

(7)

Figure 3. Deformation mechanism map for polycrystalline ice of 1·0 mm grain size.

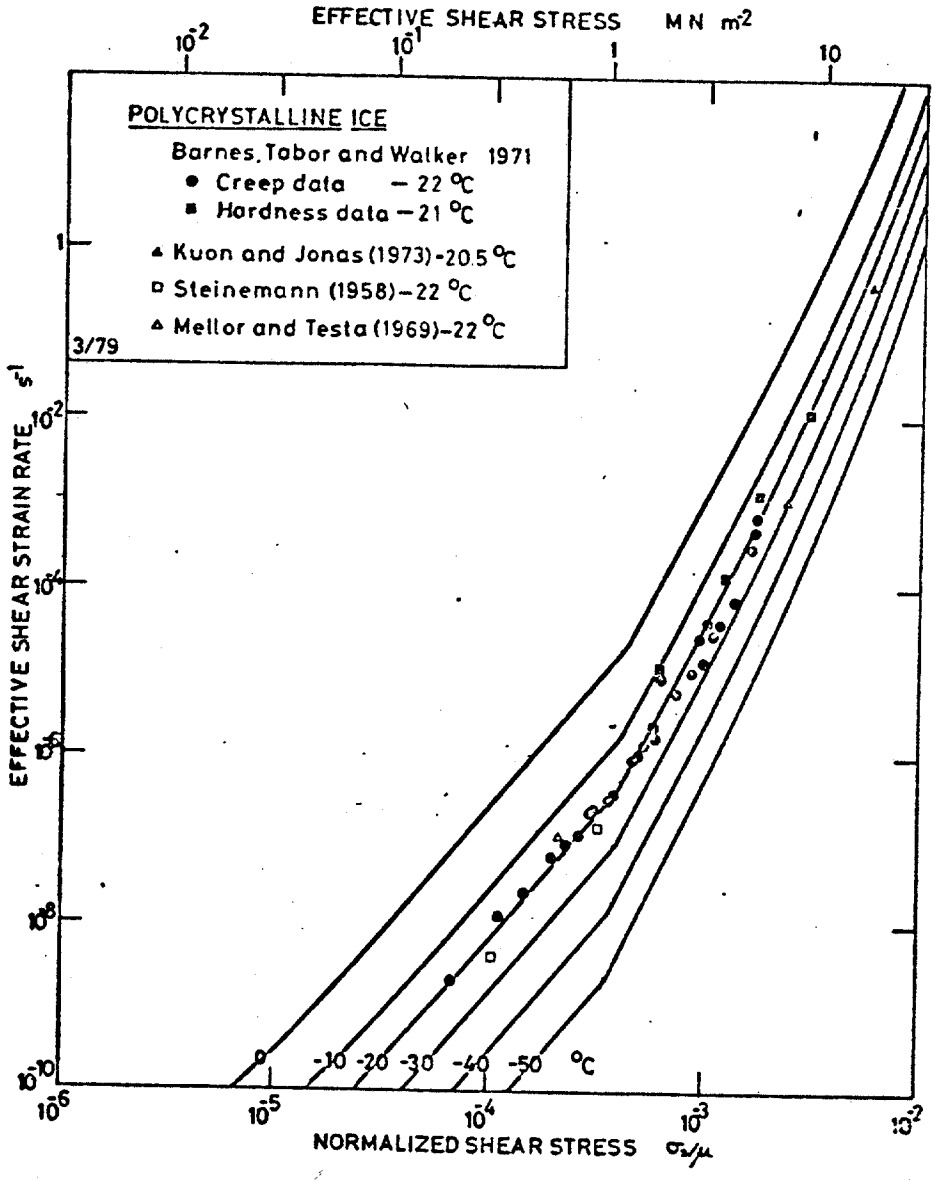

Figure 5. Constant temperature plots of the constitutive equations of Table 1 which depict dislocation glide in ice controlled by the rearrangement of protons. Two constants in the equations, σ_0 and ν_0, were determined by a least-squares fit to original data by Barnes et al (Proc. Roy. Soc. 234A (1971) 127). Taken from reference 7.

for ice. While they would not be as well based upon physics as the ones presented here (because transient strain would be modeled phenomenologically), they might have greater engineering value because all strains would be shown, including an elastic field within which the elastic strain exceeds the total plastic strain.

Implicit in the presentations of the deformation mechanism maps is the view that high rate deformation can occur without fracture. The maps, then, should really be viewed as diagrams which characterize flow when a sufficiently large hydrostatic stress, known from extrusion studies[15] to suppress fracture in ice, has been added to the effective shear stress causing flow. Also implicit is the assumption that hydrostatic pressure per se does not significantly affect the flow stress, as suggested by experiment[16] and discussed more fully in Section 6 of this report. However, pressure does lower the melting point* and, thus, indirectly affects the flow stress, as discussed in Appendix 3.

Although different, ice is not unique in all its characteristics. The compendium of maps[12] shows that, like ice, the covalently bonded substances silicon and germanium also possess small fields of diffusional creep. (Interestingly, the elements noted possess the diamond cubic crystal structure, also possessed by ice when formed by depositing water vapor onto substrates cooled below $\approx -150°C$.[17]) This characteristic reflects the fact that the diffusion coefficient in these three solids, at a given fraction of their melting points, is smaller by two to three orders of magnitude than that in every other class of solids,[18] Figure 6.

Before closing this section, it is noted that a phenomenological approach to the problem of modelling the transient and steady-state flow of polycrystalline ice has been published.[19,20] While potentially useful, such a treatment as currently developed suffers from the lack of a physical connection. Moreover,

---

*Pressure reduces the melting point of ice at the rate of 1°C for every 10 MPa.

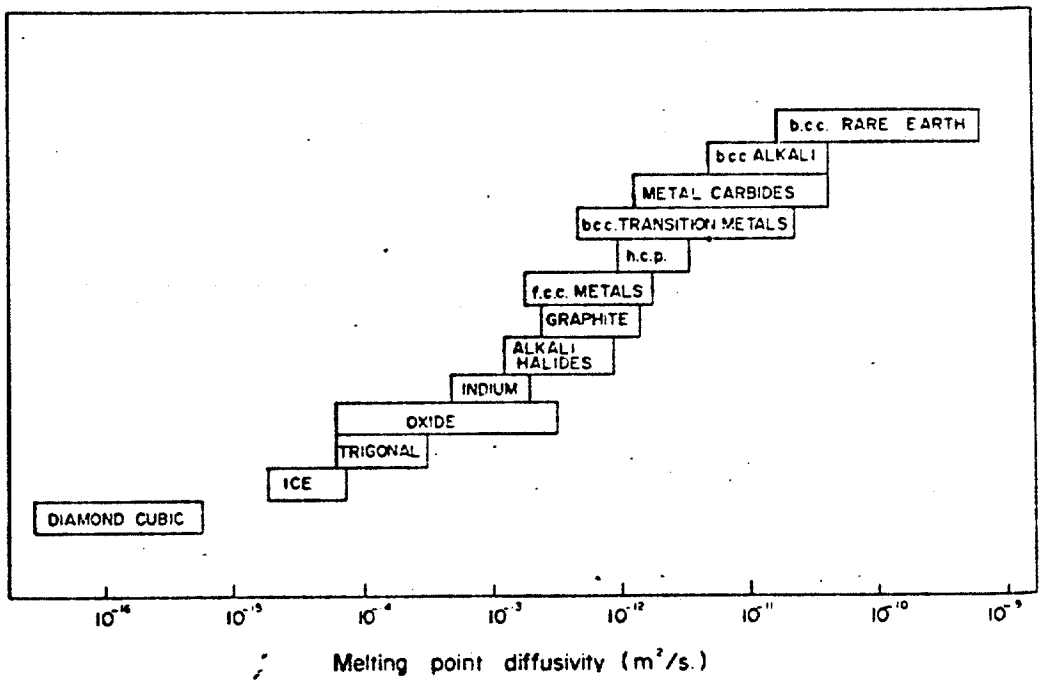

Figure 6. Melting point diffusivities for various classes of crystalline solids, taken from reference 18. Note that values for ice and the diamond cubic elements (Ge, Si) are orders of magnitude lower than those for metals.

it provides little guidance concerning the temperature/stress regime in which the proposed relations are valid, and it appears to ignore materials parameters.

To summarize, physical models of the steady state deformation of ice have recently been published and have led to constitutive relationships incorporating materials parameters. Such relationships have been used to generate deformation mechanisms maps. The maps can be used to estimate the steady state flow rate for an aggregate of specific grain size subjected to a known stress at a particular temperature. In addition, they indicate which mechanism contributes more than any other to that flow and, consequently, can be used to estimate the stress sensitivity of the flow rate at a given point in temperature-stress space. Transient maps which show the total strain accumulated for a given time at the same point in temperature/stress do not exist for ice, but could be computed.

4. STRENGTH UNDER UNIAXIAL LOADING

The purpose of this section is to consider the nature of yielding and fracture in ice loaded either in tension or in compression at a constant rate of deformation. Again, attention is focused on the behavior of equiaxed and randomly oriented polycrystals of constant grain size. Unless otherwise stated, it will be assumed that the material is free from cracks prior to loading. Uniaxial loading is considered here and multiaxial loading, in Section 7.

4.1 Tension

Consider first loading in tension. As the stress rises through the elastic region, the induced shear stress eventually reaches a point where sources of dislocations within grains or on grain boundaries begin to operate. Dislocations then start to move through those grains most favorably oriented with respect to the tensile axis (i.e. grains within which the orientation of

the basal plane is inclined at $\approx 45°$ to the tensile axis). They pile up at the boundaries with adjacent grains less favorably oriented for slip, Figure 7. Stress and elastic strain concentrations are thereby produced at the tips of such pileups. At this stage in the deformation, only localized microplasticity has occurred. Upon raising the stress, other grains less favorably oriented with respect to slip begin to deform plastically leading to more pileups. In the meantime, the stress/strain concentration at the first pileups increases, mainly through the addition of more dislocations, until it is sufficient either to nucleate a microcrack or to propagate slip into an adjacent grain. Generally, slip propagation is very difficult, and so cracks prefer to be nucleated instead. The question is: Will the cracks, once formed, propagate immediately and lead to brittle fracture? Note that we have in ice a more complicated situation than the one treated by Griffith[21] who considered the propagation (and not the initiation) of pre-existing surface or internal cracks in a purely elastic medium.

Before answering the question, it is worth repeating that at this point general plasticity has not occurred throughout the polycrystal. For hexagonal materials like ice and the metals zinc, cadmium and magnesium which slip easily only on the basal plane, general plasticity throughout polycrystalline aggregates occurs only when additional "hard" slip systems, crystallographically different from the "soft" basal ones, become active. This is because at least four independent slip systems are required for some general plasticity in such materials.[22] Slip on the basal plane provides only two. The "hard" plane in polycrystalline ice is probably the prismatic plane or a pyramidal plane. In any case, it is important to appreciate that even though general plasticity is difficult, general microplasticity is not.

Returning to the question of whether freshly nucleated cracks propagate, we invoke the concepts of fracture mechanics (considered more fully in Section 9

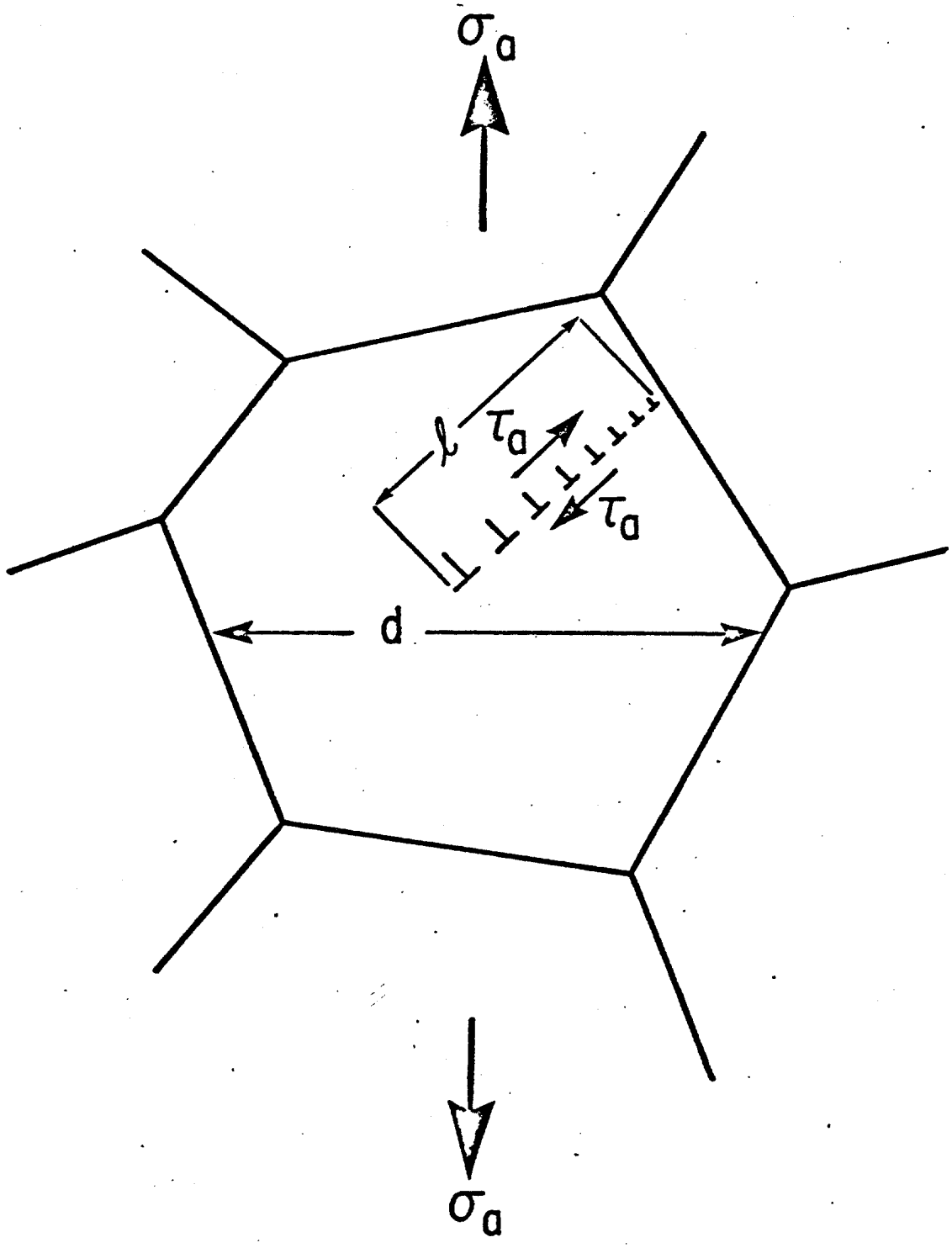

Figure 7. Sketch of a dislocation pile-up at a grain boundary in polycrystalline ice under a tensile stress σ_a. τ_a is an induced shear stress which operates the dislocation source. l is the length of the pile-up. ⊥ denotes dislocations.

of this report). Consider the stress intensity factor $K = Y \sigma_y^s \sqrt{C}$, where $Y \simeq 1$, σ_y^s is the stress to cause microyielding on the soft system and, hence, to cause crack nucleation, and C is the half-length of the given cracks and is proportional to the grain size,* d. If K exceeds a critical stress intensity factor, K_{IC}, termed the plane strain fracture toughness, then the crack propagates as soon as it is formed and brittle fracture ensues. Otherwise, the stress will have to be increased further or the cracks will have to grow (if time permits), leading to additional microplasticity and then to delayed propagation or quasi-brittle fracture. In other words, if the yield stress on the soft system exceeds the value

$$\sigma_F = \frac{K_{IC}\, d^{-\frac{1}{2}}}{Y'} \qquad (6)$$

(where Y' is another geometrical factor+) then the crack will propagate immediately after it is formed; but if $\sigma_y^s < \sigma_F$ then the crack nucleated by microslip will not propagate immediately.

This account may be furthered by noting that brittle fracture just occurs when $\sigma_y^s = \sigma_F$. An equivalent microstructural criterion may then be obtained in terms of the resistance, σ_i^s, offered by the ice lattice and its defects to the passage of slip dislocations on the soft (basal) system and in terms of the effectiveness, k_y^s, with which grain boundaries impede basal slip. Writing the yield (i.e. crack nucleation) stress in the form

$$\sigma_y^s = \sigma_i^s + k_y^s\, d^{-\frac{1}{2}} \quad , \qquad (7)$$

as recently established for ice[23] and as is commonly the case in brittle solids (e.g. NiAl,[24] iron[25] and zinc[26] at low temperatures), and by equating equations (6) and (7), the microstructural criterion is given as:[27]

---

*C is proportional to d because the wavelength of the internal stress caused by dislocations piling up at grain boundaries is about equal to d. Here, "wavelength" refers to the distance within a grain of ice over which the internal stresses reach a peak, fall, and then reach another peak.

+For penny-shaped cracks, Y' ≃ 0.6, assuming that the crack length equals d/2.

$$d_c^s = \left(\frac{Y'' K_{IC} - k_y^s}{\sigma_i^s} \right)^2 , \qquad (8)$$

where d_c^s is analogous to a critical crack size, and $Y'' = \frac{1}{Y'}$. Cracks in grains larger than d_c propagate immediately while cracks in smaller ones do not. In other words, d_c is a critical grain size: cracks formed within aggregates for which $d < d_c^s$ are stable, whereas those formed within polycrystals for which $d > d_c^s$ are not.

Figure 8 illustrates this analysis. It should be noted that even if $d < d_c^s$ general plasticity will not necessarily be observed. For such plasticity to occur, it is suggested that d must be less than d_c^h, where $d_c^h < d_c^s$ and is given as:

$$d_c^h = \left(\frac{Y'' K_{IC} - k_y^h}{\sigma_i^h} \right)^2 \qquad (9)$$

where σ_i^h and k_y^h pertain to dislocation glide on the "hard" system. Three regimes of behavior can be distinguished, based upon grain size: brittle behavior for $d > d_c^s$, quasi-brittle behavior for $d_c^h < d < d_c^s$, and even ductile behavior for $d < d_c^h$. For fresh-water ice tested in tension at -10 C at 10^{-6} s^{-1}, $K_{IC} \simeq 0.1$ MPa $\cdot$ $m^{\frac{1}{2}}$,[28,29] $\sigma_i^s = 0.6$ MPa[23] and $k_y^s = 0.02$ MPa $\cdot$ $m^{\frac{1}{2}}$,[23] giving $d_c^s \simeq 15$ mm. The critical grain size for macroscopic ductility, d_c^h, is thought to be < 1 mm,* since noticeable plasticity was not evident under the conditions cited. This result implies that $\sigma_i^h \gtrsim 2.5$ MPa, if† $k_y^s = k_y^h$, in keeping with the observations that "hard" glide in single crystals requires a level of stress about ten times that for soft glide.[30] That d_c^h is so small implies that ductile behavior in tension, at least that due solely to dislocation flow, is improbable in real ice where ultrafine grains (< 1 mm) seldom occur.

---

*The smallest grain size examined in Ref. 23.

†Equating k_y^h to k_h^s is done for convenience. Whether the equation is valid may be judged through theoretical calculations. Experimental verification is difficult.

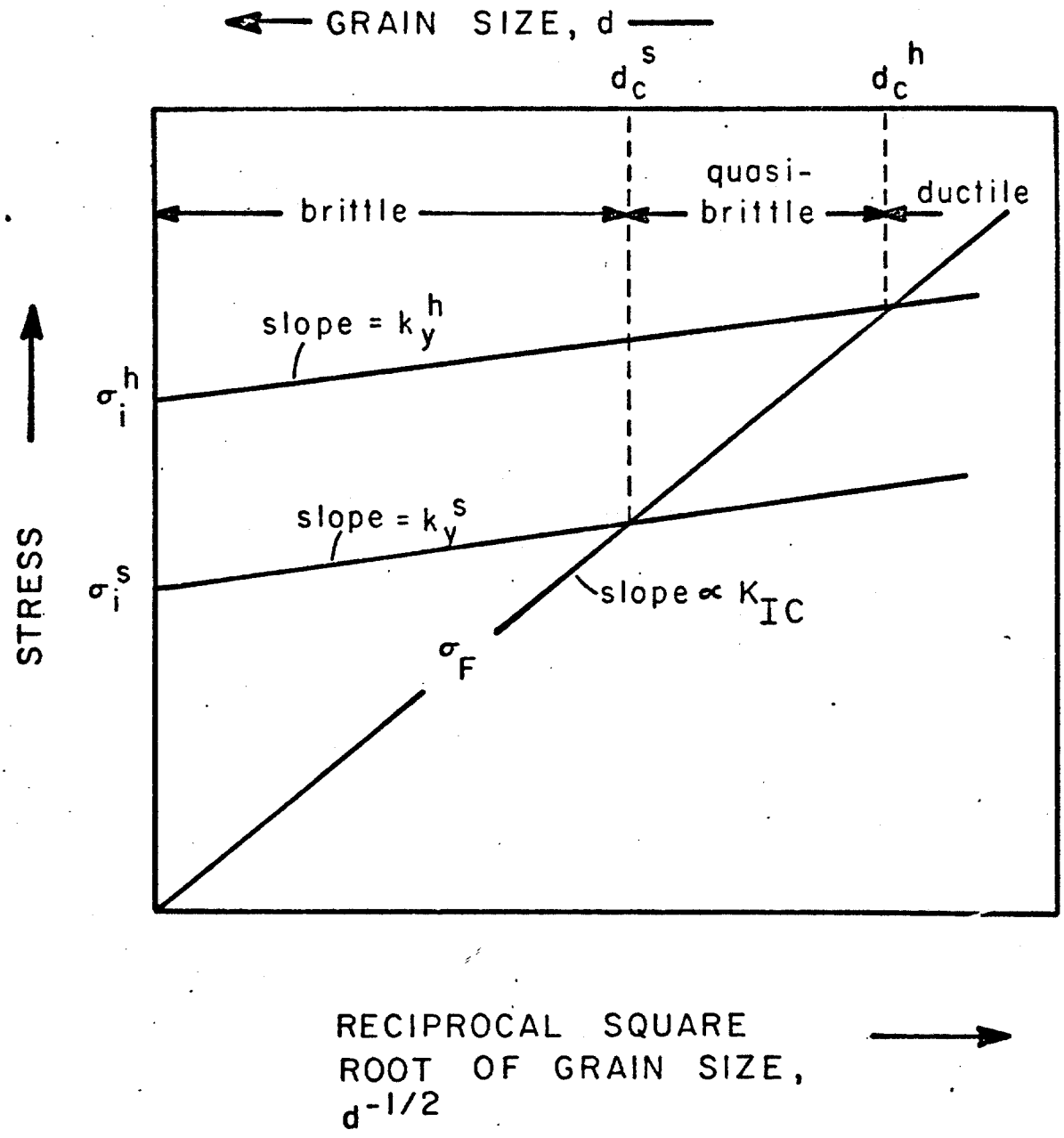

Figure 8. Sketch illustrating three proposed regions of behavior for polycrystalline ice under tension: brittle, quasi-brittle, and ductile. Brittle behavior is proposed for aggregates whose grain size is larger than d_c^s; quasi-brittle behavior for $d_c^s > d > d_c^h$, and ductile behavior for $d < d_c^h$. The parameters d_c^s and d_c^h are proposed critical grain sizes for slip on "soft" and on "hard" systems, respectively.

This analysis is an extension of one published earlier[27] and, although tentative, offers a constitutive relationship for the brittle to quasi-brittle transition in tension. The novel feature is that it incorporates both grain size and the concept of "soft" and "hard" slip systems. Thermal and rate effects are implicit, mainly through σ_i (much as they were presented earlier in connection with the constitutive equations for plastic flow) but also through variations in K_{IC}[28,29] (discussed in Section 9). If correct, the analysis suggests that the tensile strength of an aggregate of mixed grains may be determined by the average size of the largest grains within the aggregate and not by the average size of all grains.

While the foregoing discussion applies specifically to crack-free ice, the same ideas apply when dealing with the behavior of ice which is cracked prior to loading. Thus, if the cracks are smaller than d_c^s (set by the temperature and strain rate of interest), then they have little effect in reducing the strength. But if they are larger, as they would be in a coarse-grained aggregate, then they weaken the material. In this case, the strength would be given by equation (6) (i.e. the curve on Figure 8 which passes through the origin). That such predictions are credible is evident from the facts that the tensile strength of ice taken from the St. Lawrence River[31] and presumably cracked (the author's presumption) is directly proportional to $d^{-\frac{1}{2}}$, Figure 9:+ the constant or proportionality, 0.08 MPa $\cdot$ $m^{\frac{1}{2}}$, is very close to the plane strain fracture toughness of ice.[28,29]

We have, therefore, a conceptual cum quantitative basis for considering the tensile strength of ice. The question now is to consider the compressive strength.

---

*Michel[31] did not specify the temperature and strain rate. Temperature was probably $\simeq$ -10°C; strain rate is not too important for tensile behavior at rates above 10^{-6} s^{-1} at -10°C.

+The author obtained the data for Figure 9 from Michel's Figure 6.[31] Numbers are listed in Table 3.

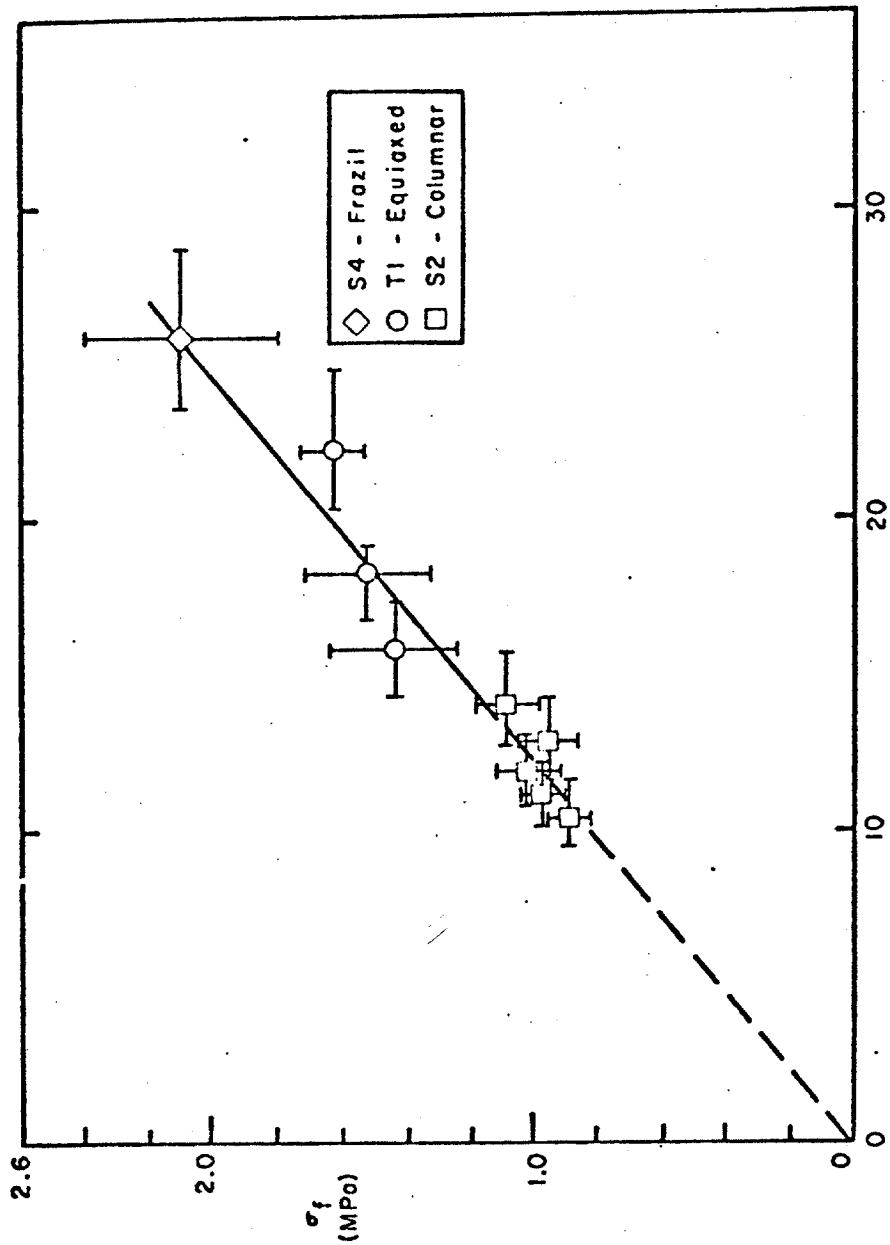

Figure 9. The tensile strength of three types of ice taken from the St. Lawrence River as a function of the recripocal square root of grain size. The data were taken from reference 31 and replotted versus $d^{-\frac{1}{2}}$. Note that the curve passes through the origin and that the slope, 0.08 MPa.$m^{\frac{1}{2}}$, is close to the plane strain fracture toughness of ice, indicating that the ice was cracked before testing and that the length of the crack was proportional to the grain size.

Table 3. Strength Data (from Michel[31]) on St. Lawrence River Ice

Grain Size, d (-m-) Esimated with ± 20% according to Michel	Type of Ice	σ_f (MPa)	No. Points	$d^{\frac{1}{2}}$ ($m^{-\frac{1}{2}}$)
$(1.5 \pm 0.3) \times 10^{-3}$	S4	2.1 ± 0.3	14	25.8
$(2 \pm 0.4) \times 10^{-3}$	T1	1.6 ± 0.1	3	22.4
$(3 \pm 0.6) \times 10^{-3}$	T1	1.5 ± 0.2	8	18.3
$(4 \pm 0.8) \times 10^{-3}$	T1	1.4 ± 0.2	2	15.8
$(5 \pm 1.0) \times 10^{-3}$	S2	1.1 ± 0.1	2	14.1
$(6 \pm 1.2) \times 10^{-3}$	S2	1.0 ± 0.1	8	12.9
$(7 \pm 1.4) \times 10^{-3}$	S2	1.0 ± 0.1	4	12.0
$(8 \pm 1.6) \times 10^{-3}$	S2	1.0 ± 0.07	3	11.2
$(9 \pm 1.8) \times 10^{-3}$	S2	0.9 ± 0.06	2	10.5

4.2 Compression

Fundamentally, the nucleation of microcracks under compressive loading occurs in the same way as it does under tension. Thus, for ice of a given grain size deformed at a given rate at a given temperature, the axial stress necessary to nucleate cracks is the same as it is in tension. The lengths of the cracks are also the same; i.e. about one-half of the grain diameter. Under combined loading, again the same value of the effective or equivalent shear stress (defined in Section 3) is required to nucleate cracks, and the same length results. The question thus turns to the stability of freshly nucleated cracks, for under compression tensile stresses are induced at crack tips.

Based upon the theory of crack propagation through a purely elastic medium (i.e. the Griffith theory), calculations[32] suggest that the compressive strength of solids containing randomly oriented cracks is 8 times the tensile strength of the same material. Under biaxial compressive loading the ratio is even greater. While this theory (with certain modifications[33]) works well for rock,[34] it has been said[35] not to apply for ice for which the ratio of the compressive to the tensile stress, σ_C/σ_T, to cause fracture is closer to 5 or smaller.[36]

It is not surprising that $\sigma_C/\sigma_T < 8$, at least for "warm" ice; i.e. ice fractured around -10°C or so. At these temperatures, ice is capable of plastic flow (as demonstrated by creep tests) and, therefore, is not the purely elastic solid for which the theory is intended. Another reason, probably the more important, is that the theory is strictly applicable to crack propagation. As we saw in Section 4.1, propagation cannot occur until cracks are nucleated; in tension the stress to nucleate cracks is higher than the stress to propagate them, thereby effectively lowering the ratio of compressive to tensile strength. This explanation could be checked experimentally by testing at high strain rates ($\gtrsim 10^{-3}$ s^{-1} at -10°C) pre-cracked ice in tension and in compression. Rather than elaborating further on the σ_C/σ_T ratio, however, our purpose now is to consider the stress/strain curve in compression.

Figure 10[13] illustrates a typical curve for low deformation rates ($\lesssim 10^{-4}$ s^{-1} at -10°C). The first inflection corresponds closely to crack nucleation, evident from acoustical[37] emissions accompanying its occurrence. This we call the yield point. Could the cracks have propagated immediately (in an elastic fashion) under the tensile stress induced at their tips? On the basis of crack propagation in tension, discussed above, and by incorporating the elastic theory, a critical crack length in compression may be estimated from the expression:

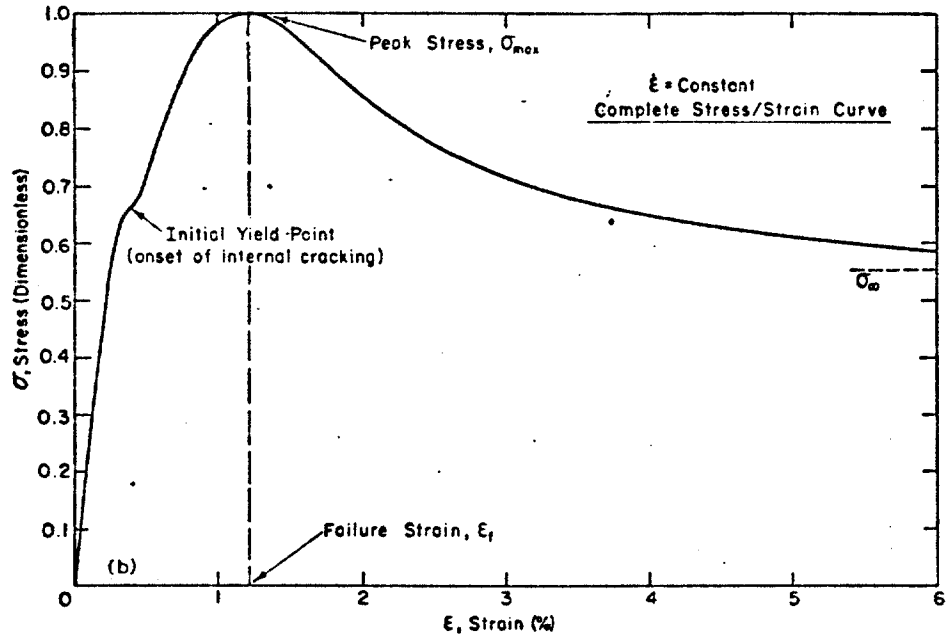

Figure 10. Idealized stress/strain curve for polycrystalline ice slowly deformed at a constant strain rate. (Taken from Ref. 13)

$$2c_c = \frac{d_c}{2} = \frac{1}{2}\left(\frac{\lambda Y'' K_{IC} - k_y^s}{\sigma_i^s}\right)^2 \qquad (10)$$

where $\lambda \geq 8$ is the ratio of the compressive to tensile strength as determined by crack propagation.* This exceeds about 850 mm for low rate deformation (10^{-6} s^{-1}) at -10°C (using the same K_{IC}, k_y^s and σ_i^s as given above)! Clearly, cracks this size are just not permitted in laboratory tests, implying that true brittle fracture under uniaxial compression is highly improbable in experimental situations.

Note that the so-called "brittle fracture" which occurs in compression[36,38] at deformation rates higher than about 10^{-3} to 10^{-2} s^{-1} is then not really brittle fracture in the strict sense. It is fracture via a brittle mode which occurs once the compressive stress has risen sufficiently to propagate the cracks nucleated by microplastic flow on the soft slip system. In other words, microplasticity in addition to that required to nucleate the cracks in the first place probably occurs before the material becomes sufficiently highly stressed to fracture.

Returning to the stress/strain curve, the stress continues to rise after cracks begin to nucleate, but probably does not reach the level needed to activate general slip on the "hard" system (about ten times as hard as the basal system[30]). The strain hardening which is apparent is then considered to be largely elastic in nature, originating in the elastic deformation of grains less favorably oriented with respect to slip but within which microplastic flow has occurred. During hardening, the cracks originally nucleated may grow, if the deformation rate is low enough, while new ones form. Microstructurally, the number density of microcracks increases and the load bearing area decreases.

The foregoing comments suggest that if the stress were held constant at some level between the yield point and the peak stress, crack growth may occur, leading eventually to fracture. From a practical point of view,

---

*When nucleated under uniaxial compressive loading, cracks are not randomly oriented. Rather, they are aligned more or less along the compressive axis. For this reason λ exceeds 8, approaching values as high as 15 or higher for cracks aligned around 10° or closer to the loading direction.

"creep crack growth", if real, could lead to lower ice-induced forces on engineered structures when the movement of an ice sheet is interrupted.

What accounts for the peak stress? Microstructural softening, such as the development of a preferred orientation (most recently reported[39] in ice compressed in plane strain at -1°C) or dynamic recrystallization (also known to occur in ice[40] and seen in metals[41] strained above 65% of their melting points), is improbable for two reasons. Firstly, the magnitude of the strain prior to softening is only about 0.01 (i.e. ≃ 1% shortening] at which level neither preferred orientation develops,[39] at least at -1°C, nor is recrystallization to be expected. And, secondly, the axial stress corresponding to the onset of microstructural softening should not be significantly increased by hydrostatic pressure, whereas the peak stress is (discussed in Section 6). More probable is a mechanism related to the combination of cracking and dislocation slip, cracking so intensifying the shear stress within localized regions around the cracks that both "hard" and "soft" slip may operate. According to such a mechanism, general plasticity via the "hard" and "soft" systems becomes possible when the volume fraction of cracks reaches a critical level. The softening which follows might then be caused by the rapid multiplication of slip dislocations and thus by the requirement of a lower applied stress to maintain the strain rate, $\dot{\gamma}$. In other words, because $\dot{\gamma} = \rho b v$, where ρ is the mobile dislocation density, b is the dislocation Burgers vector, and v is the dislocation velocity, and because v decreases as stress decreases, then as ρ increases, the flow stress decreases. Hydrostatic stress suppresses cracking, and so higher levels of applied stress are needed to activate the combined flow processes. That dislocation slip plays a significant role on the down-hill side of the stress/strain curve is evident

from the strain-rate sensitivity of the down-hill stress: an incremental increase in rate increases this stress.[36]

This is not to say that cracking ceases to be a strain-producing mechanism once the peak stress is reached. Rather, the rate of cracking probably falls off on the down-hill side because an additional strain-producing mechanism -- i.e. hard slip -- is now thought to be operating locally.

At high strain rates, a higher level of stress is probably required to activate the "hard" system. Moreover, there is less time for dislocation processes to relax the stress at the tips of cracks. Consequently, the stress intensity at crack tips probably reaches the critical value before "hard slip" is activated. As a result, fracture occurs before a peak is reached. This explanation implies that hydrostatic pressure, by inhibiting crack propagation, should allow a peak stress at high deformation rates. Results supporting this suggestion have recently been published.[42]

Ostensibly, the strain rate distinguishing "brittle" from "ductile" behavior might be expected to decrease with decreasing temperature. However, because K_{IC} increases with decreasing temperature (unusual, but evidently true, as discussed in Section 9), the transition rate is not expected to be highly thermally sensitive, as observed,[38] Figure 11.

Thus, this physical interpretation, tentative though it is, accounts qualitatively for the occurrence of the peak stress in compression. It suggests that the magnitude of the peak might be lessened should a period of "creep crack growth" be permitted before loading is resumed. Moreover, it suggests that the transitional strain rate from brittle to ductile behavior and the attendant peak stress will increase with hydrostatic pressure, in keeping with two points recently observed. How good the explanation really is, however, can only be judged through systematic experimentation and by more detailed modelling.

Figure 11. Graphs of the maximum or peak strength in compression (i.e. peak stress of Figure 10) versus strain rate as a function of temperature (taken from Reference 38):

a) frazil ice
b) snow ice
c) columnar ice loaded in a direction perpendicular to the columns

11. (a) GLACE DE FRASIL

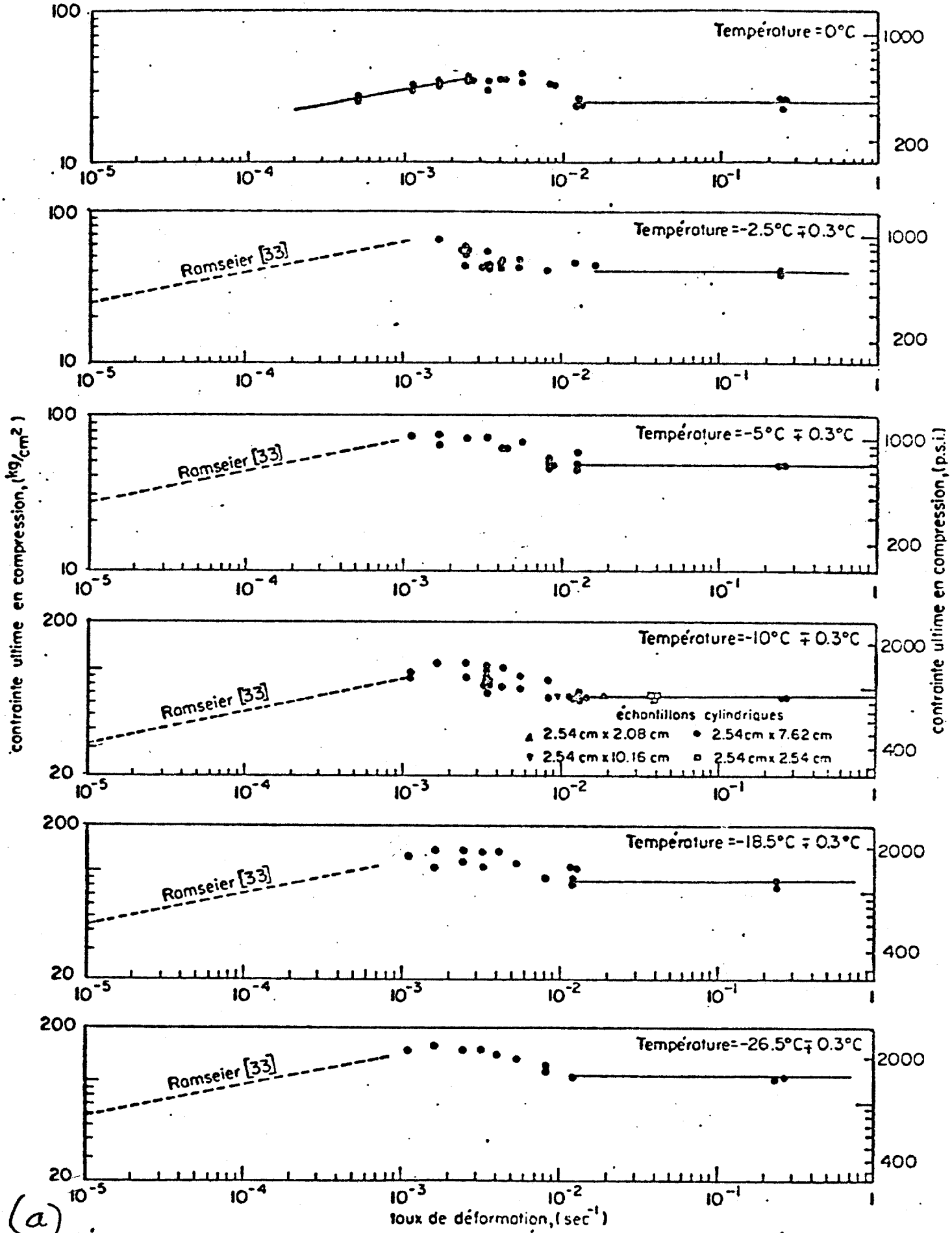

(a) RÉSISTANCE MAXIMALE EN FONCTION DE LA TEMPÉRATURE ET DU TAUX DE DÉFORMATION

11. (b) GLACE DE NEIGE

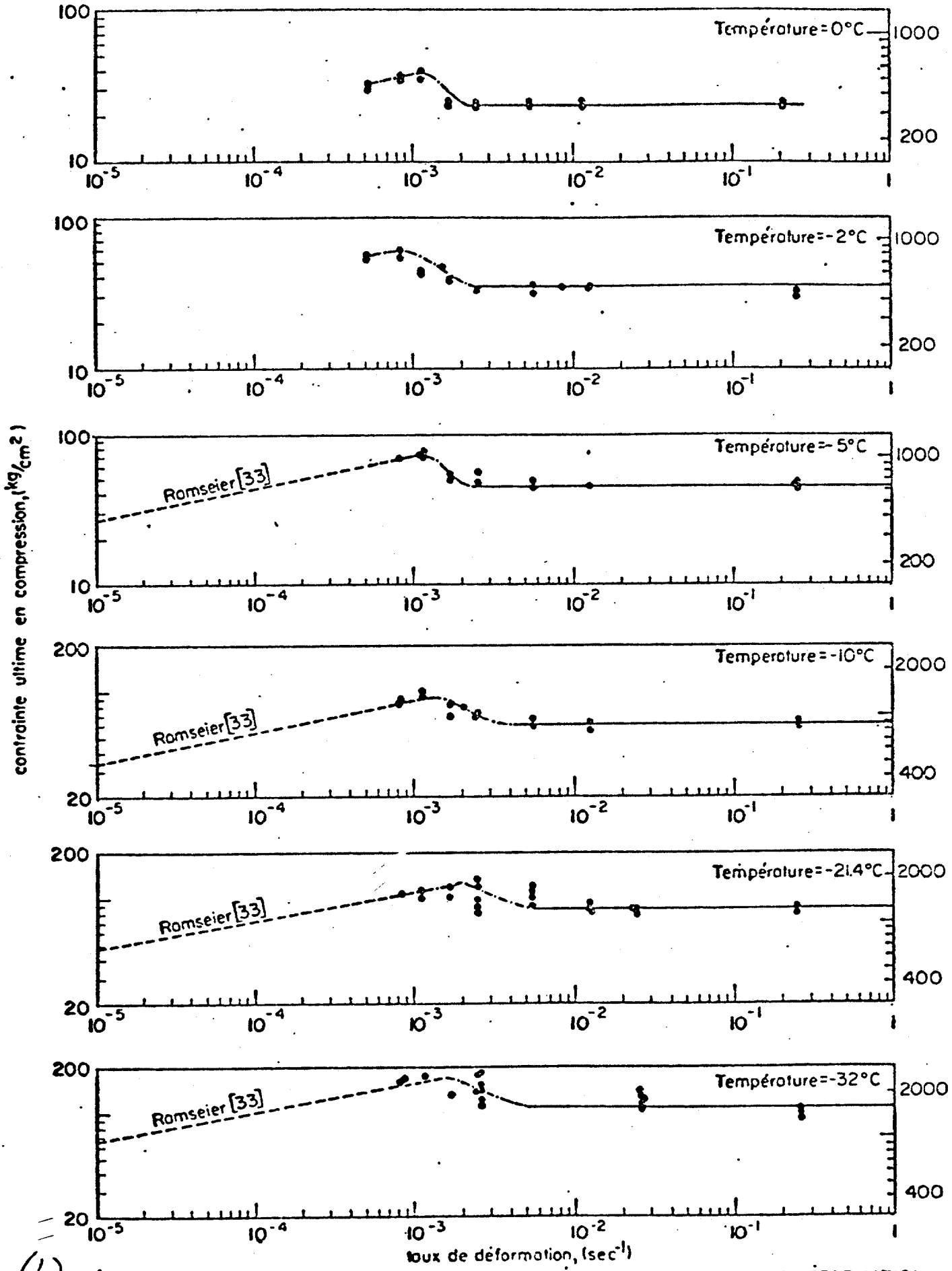

(b) RÉSISTANCE MAXIMALE EN FONCTION DE LA TEMPÉRATURE ET DU TAUX DE DÉFORMATION

II. (c) GLACE COLUMNAIRE (S2)

échantillons horizontaux prélevés à 10 cm sous la surface

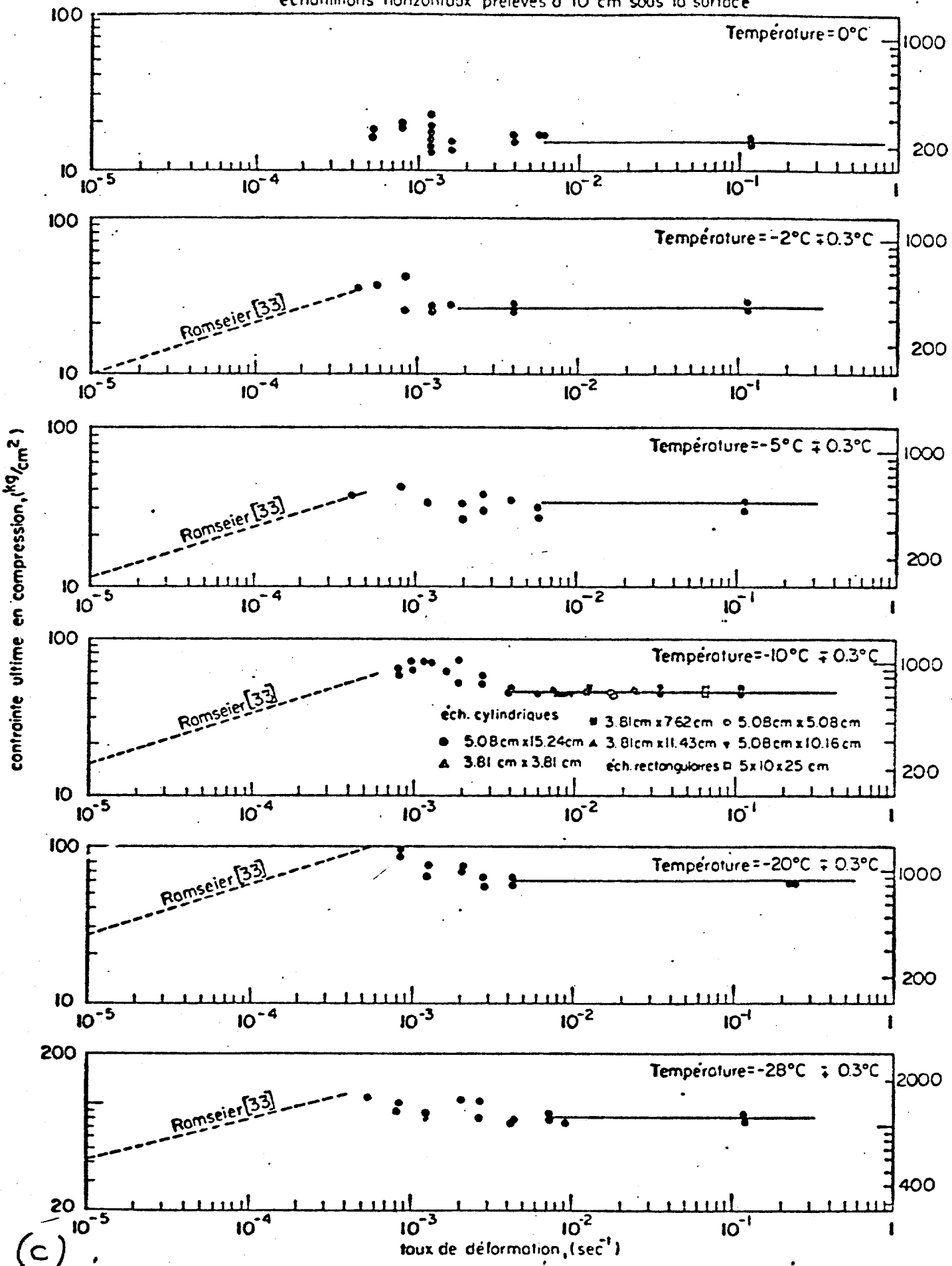

(c) RÉSISTANCE MAXIMALE EN FONCTION DE LA TEMPÉRATURE ET DU TAUX DE DÉFORMATION

5. FURTHER COMMENTS ON GRAIN SIZE EFFECTS ON STRENGTH

In Section 4.1 it was noted that grain refinement increases the tensile strength of ice and, although improbable in practice, may impart a small amount of macroscopic plasticity in tension. Here, attention is focused on the effects of grain size on the compressive strength, σ_c, taken as the maximum peak stress obtained at low strain rates (Section 4.2).

Two series of experiments, one[43] on granular ice and the other[44] on columnar ice (S2 type), suggest that σ_c, like the tensile strength, increases as the average grain size, d, decreases. For instance, at -10°C and 10^{-5} s^{-1}, σ_c increases from 2 MPa for d = 10 mm to 3.8 MPa for d = 1mm, independent of the type of ice. Again, the functional relationship is of the type:

$$\sigma_c = \sigma_i^c + k_y^c d^{-\frac{1}{2}} \qquad (11)$$

where, for the conditions noted, σ_i^c = 1 MPa and k_y^c = 0.1 MPa$\cdot m^{\frac{1}{2}}$. Both σ_i^c and k_y^c are larger than their counterparts in the relationship for tensile strength (equation 7, page 20 and 21), probably because different levels of plastic strain were incorporated in the evaluation of the parameters in the two cases; i.e. 3×10^{-4} versus $\simeq 10^{-2}$ compression.

These experiments suggest that grain refinement significantly increases the crushing strength of ice. Others, on the other hand, suggest that grain size has no effect. Sixty-two experiments[45] on aggregates of granular ice having grains averaging from 0.5 to 2 mm in diameter reveal no consistent variation in strength with grain size, but indicate instead a maximum stress of 7.5 $\pm$ 1 MPa at -10°C at 5×10^{-4} s^{-1}.

Why the difference? One possibility is that the ratio of grain sizes was different -- i.e. approximately an order of magnitude in one case[43] but only a factor of four in the other.[45] Yet, even a factor of three in grain size (from d = 6 mm to d = 2 mm) indicated a strengthening effect,[44] eliminating the suspicion of the ratio of largest/smallest grain per se.

5. FURTHER COMMENTS ON GRAIN SIZE EFFECTS ON STRENGTH

In Section 4.1 it was noted that grain refinement increases the tensile strength of ice and, although improbable in practice, may impart a small amount of macroscopic plasticity in tension. Here, attention is focused on the effects of grain size on the compressive strength, σ_c, taken as the maximum peak stress obtained at low strain rates (Section 4.2).

Two series of experiments, one[43] on granular ice and the other[44] on columnar ice (S2 type), suggest that σ_c, like the tensile strength, increases as the average grain size, d, decreases. For instance, at -10°C and 10^{-5} s^{-1}, σ_c increases from 2 MPa for d = 10 mm to 3.8 MPa for d = 1mm, independent of the type of ice. Again, the functional relationship is of the type:

$$\sigma_c = \sigma_i^c + k_y^c d^{-\frac{1}{2}} \qquad (11)$$

where, for the conditions noted, σ_i^c = 1 MPa and k_y^c = 0.1 MPa$\cdot m^{\frac{1}{2}}$. Both σ_i^c and k_y^c are larger than their counterparts in the relationship for tensile strength (equation 7, page 20 and 21), probably because different levels of plastic strain were incorporated in the evaluation of the parameters in the two cases; i.e. 3×10^{-4} versus $\simeq 10^{-2}$ compression.

These experiments suggest that grain refinement significantly increases the crushing strength of ice. Others, on the other hand, suggest that grain size has no effect. Sixty-two experiments[45] on aggregates of granular ice having grains averaging from 0.5 to 2 mm in diameter reveal no consistent variation in strength with grain size, but indicate instead a maximum stress of 7.5 $\pm$ 1 MPa at -10°C at 5×10^{-4} s^{-1}.

Why the difference? One possibility is that the ratio of grain sizes was different -- i.e. approximately an order of magnitude in one case[43] but only a factor of four in the other.[45] Yet, even a factor of three in grain size (from d = 6 mm to d = 2 mm) indicated a strengthening effect,[44] eliminating the suspicion of the ratio of largest/smallest grain per se.

Another is that the range of sizes differs significantly: the range 0.5 to 2 mm contains fine grains which probably grow[+] to around 1 mm during storage at -10°C, thereby reducing the effective range investigated; the range 1 mm to 10 mm contains relatively stable grains. A third possibility, less likely than the second, is that the strengthening effect noted at a strain rate of 10^{-5} s^{-1} is suppressed upon increasing the deformation rate by a factor of 50.

Incidentally, conflicting results concerning grain size effects on the strength of ice have also been reported in relation to creep deformation. One set[(46)] suggests a rather complicated behavior in which the creep rate first decreases and then increases upon increasing grain size from 0.7 to 2 mm. The other set[(47)] indicates no change over a range of grain size from 1 to 10 mm. This conflict probably reflects some uncertainties about the first set of experiments: it is not clear that secondary creep was actually measured, nor is it clear that a sufficient number of grains (as few as five across the diameter) comprised the smallest dimension of the test specimens.

Clearly, uncertainties exist. Until they are clarified through further research, it is suggested that the possibility of increasing the compressive strength of ice through grain refinement be kept in mind when interpreting data. In so doing, it should be noted whether variations in the average grain size are accompanied by variations in the degree of preferred orientation or fabric, for if they are, one effect could camouflage the other.

6. THE COMPRESSIVE STRENGTH UNDER HYDROSTATIC PRESSURE

There appears to be some confusion in the literature concerning the role of hydrostatic pressure on the strength of ice. Rigsby,[(16)] for instance, concluded from creep studies on single crystals that hydrostatic pressure has no effect on the rate of deformation, provided that temperature is measured from the pressure-melting point.* Jones,[(42)] on the other hand, recently reported

*Recall that the melting point of ice decreases by 1°C per 10 MPa of hydrostatic pressure. See appendix 3.

[+]Appendix 4 notes reported data which strongly suggest that grain growth occurs at -1(

that the peak strength of equiaxed and randomly oriented polycrystals compressed at 5.5×10^{-3} s^{-1} at -11°C is increased from 11 to 21 MPa upon raising the confining pressure from one atmosphere to 34 MPa. How, in one case, can hydrostatic pressure not affect mechanical behavior, yet in another have a significant effect?

The answer probably resides in the fact that the two sets of experiments measured different responses. In Rigsby's case, plastic flow was occurring. His experiments, then, show that the effective shear stress necessary to maintain flow at a given rate is independent of the hydrostatic component of the stress tensor. In other words, the ease with which dislocations glide in ice -- i.e. the ease with which this type of strain-producing mechanism operates -- appears not to be significantly affected by stress normal to the slip plane, in keeping with the behavior of most crystalline solids. In Jones' case, on the other hand, the pressure probably retarded the growth of cracks which nucleated at the yield point (as discussed in Section 4), thereby decreasing the total volume fraction of cracks. As a result of fewer stress-producing defects, higher applied stresses are required to activate slip of the "hard" system necessary for general plastic flow of the aggregate at high rates. In keeping with this explanation is the observation[48] that highly confined specimens contain far fewer cracks (as seen by eye) than unconfined ones shortened by the same amount ($\simeq$ 7%).

Incidentally, at -10°C, the effect of hydrostatic pressure beins to drop off for pressures above 34 MPa (at least for rates around 5.5×10^{-3} s^{-1}), owing to pressure melting. Presumably, at lower temperatures where the reduction in the melting point by pressure does not bring ice so close to melting, hydrostatic effects will continue to higher levels of stress and even greater strengthening will result.

It should be noted that under confinement ice can be shortened by 50% without falling apart. This limit is a machine limitation and not a materials

one,[48] implying that further deformation is possible. This result is reminiscent of the observation that ice can be extruded,[15] noted earlier, and that even marble can.[49] It suggests that under suitable conditions, sea ice moving against stationary objects may flow rather extensively.

Thus, hydrostatic pressure is expected to increase the maximum load-bearing capacity if ice is compressed at rates where relaxation near cracks is small, and to impart greater ductility. At lower rates ($< 10^{-5}$ s^{-1}), hydrostatic pressure will probably be less effective because here relaxation rates are rapid enough to permit plastic flow without requiring "hard" slip.

7. STRENGTH OF ICE UNDER MULTIAXIAL LOADING

From the foregoing discussion it is clear that the maximum forces exerted by moving ice against stationary objects will be larger where the ice is in a state of triaxial compression than when it is uniaxially stressed. How much larger will probably depend not only on the magnitude of the triaxial compression, but also on the ratio of the principal stresses and on the type of ice (i.e. columnar vs. granular). This section considers explicitly the effects of general multiaxial compressive loading (as opposed to $\sigma_2 = \sigma_3$ in the hydrostatic case), particularly on the strength of S2 type columnar ice.

S2 ice is comprised of columnar grains aligned parallel to the growth direction in which the C-axes are randomly oriented within the plane normal to the growth direction. This material, like equiaxed and randomly oriented granular ice, exhibits a peak in strength when it is uniaxially compressed slowly in a direction perpendicular to the columns.[50] It also displays a peak when multiaxially compressed.[51]

How large is the peak stress for a given stress ratio? Based upon the explanation presented in Section 4.2, we expect that the magnitude reflects the ease of slip and is a measure of a critical shear stress induced either through the application of an externally applied stress only or through the

combined effects of an external stress and the stress-concentrating action of a critical number of cracks.

With this idea in mind, and with the thought that material so highly textured as S2 ice may undergo extensive flow on only a single slip plane, the recently published[51] multiaxial compressive strengths for artifically grown S2 saline ice were analyzed. The raw data are listed in Table 4 and pertain to material comprised of columns of 5 to 20 mm in "diameter"* and deformed at -10°C at 2×10^{-4} S^{-1}. In each case (numbered 1, 2, 3 ...) the ratio of the three principal stresses $\sigma_1 : \sigma_2 : \sigma_3$ remained constant. σ_1 was applied along the axis of the columns, and σ_2 and σ_3, perpendicular to the columns. Also listed are the maximum shear stresses acting on the basal ("soft") and on the prismatic ("hard") systems at the point when the peak in stress was reached. These shear stresses were computed from the differences in the principal stress; i.e. from $(\sigma_2 - \sigma_3)/2$ for the basal system and from the larger of $(\sigma_1 - \sigma_2)/2$ and $(\sigma_1 - \sigma_3)/2$ for the prismatic system. Interestingly, the peak in stress correlates fairly well with either a shear stress on the basal system of 1.4 ± 0.2 MPa or with a shear stress on the prismatic system of 4.9 ± 0.8 MPa. (The "active" system is suggested in Table 4.) The only exception is case No. 22; the only hole is case No. 16, the pure hydrostatic case for which a peak is not expected and for which it is uncertain as to whether one was observed.

It appears, therefore, that we can at least estimate the peak stress knowing the ratio of $\sigma_1:\sigma_2:\sigma_3$ and by invoking the critical shear stress hypothesis. However, in so doing, cognizance must be taken of the likelihood that the critical stress will increase with decreasing temperature, with increasing strain rate, and with decreasing grain size, and that the sensitivities will differ for the two systems. In other words, the numbers deduced above -- i.e. 1.4 MPa for the "soft" system and 4.9 MPa for the "hard" one --

*The diameter of the column is regarded as the diameter of the largest inscribed sphere.

Table 4. Multiaxial Compressive Strength of Saline Ice at -10°C and 2×10^{-4} s^{-1}
(data from Ref. (51))

Data								Analysis		
		Ratio of Stresses			Failure Stresses (MPa)			Maximum Shear Stress at Failure (Peak) (MPa)		Active System
Case	Code	σ_1	σ_2	σ_3	σ_1	σ_2	σ_3	Basal System	Prismatic System	B = Basal P = Prismatic
1	300	1	0	0	10.05	0	0	0	5.0	P
2	030	0	1	0	0	2.06	0	1.03	0	B
3	310	1	0.33	0	12.44	3.72	0	1.36	6.22	B & P
4	320	1	0.67	0	6.30	3.46	0	1.73	3.15	B
5	330	1	1	0	2.48	2.47	0	1.24	1.24	B
6	130	0.33	1	0	0.73	2.10	0	1.05	0.36	B
7	230	0.67	1	0	1.84	2.73	0	1.36	0.92	B
8	031	0	1	0.33	0	3.46	1.19	1.13	1.73	B
9	032	0	1	0.67	0	6.98	4.72	1.13	3.49	B & P
10	033	0	1	1	0	9.36	9.40	0.02	4.7	P
11	311	1	0.33	0.33	17.33	5.77	5.85	0.04	5.8	P
12	321	1	0.67	0.33	15.73	10.36	5.39	2.48	5.2	B & P
13	331	1	1	0.33	4.49	4.49	1.54	1.48	1.48	B
14	322	1	0.67	0.67	18.54	13.20	12.50	0.35	3.02	P
15	332	1	1	0.67	8.65	8.65	5.83	1.41	1.41	B
16	333	1	1	1	14.18	14.20	14.25	0	0	-
17	131	0.33	1	0.33	1.26	3.74	1.28	1.23	1.24	B
18	132	0.33	1	0.67	2.78	8.23	5.50	1.36	2.73	B
19	133	0.33	1	1	5.79	17.12	17.07	0.03	5.7	P
20	231	0.67	1	0.33	3.65	5.45	1.86	1.80	0.9	B
21	232	0.67	1	0.67	5.44	8.15	5.51	1.32	1.36	B
22	233	0.67	1	1	7.73	11.62	11.63	0	1.95	?

apply only at -10°C at rates of $\simeq 2 \times 10^{-4}$ S^{-1} for columnar ice 5 to 20 mm in "diameter".

Before closing this section, it is relevant to note the magnitude of the effect of multiaxial loading on the strength of the columnar saline ice described above and tested under the conditions cited. Under symmetrical loading in the plane of the sheet -- i.e. perpendicular to the growth direction -- the strength reaches 4.7 times the in-plane uniaxial compressive strength (compare cases 10 and 2, Table 4). Under symmetrical biaxial loading in the plane of the sheet plus compression parallel to the growth direction, the strength climbs to 8.5 times the in-plane uniaxial strength (compare cases 19 and 2, Table 4).

The effect of triaxial stress on the compressive strength of columnar ice is large, and should be investigated for a wide range of temperatures and strain rates. In so doing, the concept of a critical shear stress might be kept in mind as a "working hypothesis" and used both as a guide to forming the test matrix and as an aid to interpretation.

8. SURFACE AND GEOMETRICAL EFFECTS ON STRENGTH

So far, no mention has been made of artifacts. In mind here are possible effects on tensile strength due to surface condition and possible effects on both tensile and compressive strength due to too few grains across the smallest dimension of a test specimen. This section considers such possibilities.

8.1 Surface Condition

Ice may be regarded as a ceramic and like many ceramics possesses considerable strength up to high fractions of its melting point. Indeed, when its strength is normalized with respect to its shear modulus and then compared with that of other solids at the same homologous temperature (i.e. at the same fraction of the absolute melting point), ice is seen to be one of the strongest solids.[7] Yet, like many ceramics, ice is macroscopically brittle up to its melting point. Given these parallels, one wonders whether ice might

be similar to ceramics in still another way -- namely in terms of the sensitivity of tensile strength to surface condition.

Figure 12 illustrates the point in mind for magnesia and shows the effect of machining damage on the room-temperature tensile strength of this ceramic, as a function of grain size.[52] Coarse-grained material ($d > 0.1$ mm) is highly sensitive, so much so that mechanical machining (turning, grinding, etc.) reduces the strength by almost one order of magnitude. The sensitivity decreases with decreasing grain size to the extent that it becomes negligible for aggregates of grains finer than about 10 μm. This effect is caused by the generation of surface microcracks and by the pull-out of grains which act as stress raisers. The $d^{-\frac{1}{2}}$ dependence (not unlike that of ice[23] (Section 4.1) and noted in Figure 12) is a manifestation of the fact that the tensile strength is governed by the plane strain fracture toughness, K_{IC}, and by the length of the cracks (proportional to d).

Significantly, the reduction in strength due to machining can be lessened by annealing the machined surfaces. This treatment blunts the damage features so that they are much less effective as stress raisers.

How probable is a reduction in tensile strength of polycrystalline ice due to machining? Without measurements, definitive statements are difficult to make. It seems reasonable to expect, however, that some effect may exist. How long it will exist after the surface has been machined (say, cutting in a lathe at -20°C), is another question. If the material is tested immediately after machining, then the probability for an effect would seem to be rather high. On the other hand, if the surface is allowed to anneal, then the probability of a measurable effect is much lower.

How long should the surface be annealed, say at -10°C? Since blunting is a diffusion controlled process (probably, surface diffusion), it seems reasonable to expect that if the product $\sqrt{D_S t}$* for ice is made similar to

*D_S is the surface diffusion coefficient; t is time.

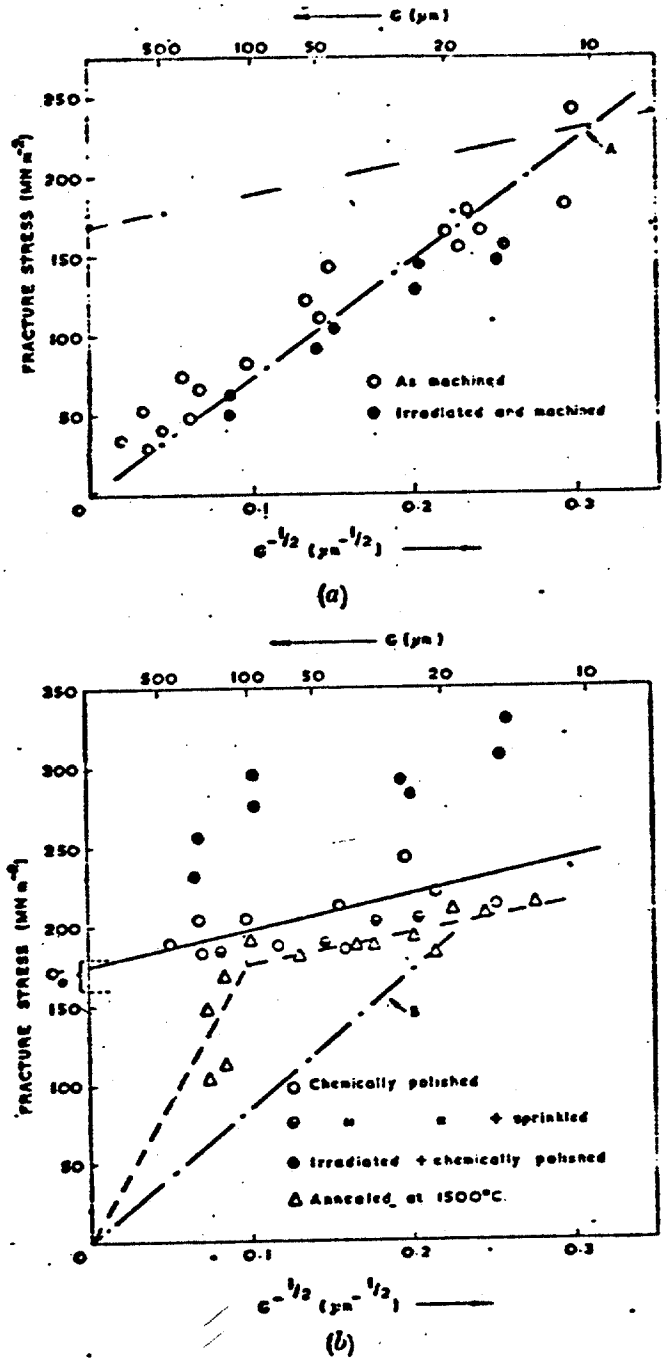

Figure 12. Fracture stress versus reciprocal square root of grain size for irradiated and unirradiated material; (*a*) machined surfaces, (*b*) chemically polished and annealed surfaces. Curves A and B represent the stresses to extend penny-shaped flaws of diameter $G/2$ and G respectively. (52)

that employed in ceramics technology, then similar benefits might accrue. For ceramics, D_S may be estimated from the volume diffusion coefficients by assuming that the activation energy, Q_S, for surface diffusion is one-half of that for volume diffusion, and by assuming that the pre-exponential term in the diffusion equation ($D_S = D_0 e^{-Q_S/kT}$) is the same in both cases. In so doing, the results listed in Table 5 were obtained using data for MgO[52] and ZnO.[53] Interestingly, in both cases $\sqrt{D_S t}$ is of the same order of magnitude as the grain size, d, suggesting that a suitable criterion for thermal annealing is:

$$\sqrt{D_S t} = d \qquad (12)$$

(The author does not know whether this or a similar criterion is employed by ceramicists.) Applying this criterion to ice of d = 10 mm annealed at -10°C yields an annealing time of:

$$t = \frac{d^2}{D_S^{ice}} = \frac{(10 \times 10^{-3})^2 \ (3600^{-1})}{10^{-3} \exp \frac{-30{,}000}{263 \times 8.4}} = 22 \text{ hours.}$$

D_S^{ice} was taken from the literature[54] assuming, as above, that the activation energy for surface diffusion is one-half that for bulk diffusion and that the pre-exponential constant in the diffusion equation is the same as it is for bulk diffusion.

Table 5. Calculated Values of $\sqrt{D_S t}$ for Annealed Ceramics

Material	Q_{bulk} (kJ/mole)	D_0 (m^2/sec)	Anneal Conditions T (°C)	t (h.)	$\sqrt{D_S t}$ (μm)
ZnO	395	1.05×10^{-5}	1100	35	22
MgO	640	10^{-3}	1500	3	72

Q_{bulk} = activation energy for diffusion; A and D_0 are obtained from Ref. (18). D_0 for MgO is the author's estimate.

Without experimentation, the quality of this estimate -- indeed the existence even of a deleterious effect of machining damange on tensile strength -- cannot be judged. However, until such time that results become available, it seems prudent to assume the worst and to allow at least one day at -10°C before testing ice in tension.

8.2 Ratio of Sample to Grain Size

From recent experiments on equiaxed and randomly oriented fresh-water ice of 1 mm grain size deformed in compression at -10°C at 5.5×10^{-4} s^{-1} (nominal), it was claimed[45] that for cylindrical specimens, 12 or more grains across a diameter (not per cross-sectioned area) are required to avoid an effect of sample size on the peak strength. The data in Figure 13 are the basis for this claim. Curiously, the curve as published suggests that the effect of too few grains is to increase the strength, presumably before it drops off to a value set by the strength of a single crystal.

Whether the claim is valid is left for the reader to judge. In any case, it seems reasonable to allow ten or more grains across the smallest dimension of a test specimen to obtain a measure of strength unaffected by the ratio of sample to grain size.

9. FRACTURE MECHANICS

From the discusson on the uniaxial and multiaxial loading of ice, it appears that cracks play a significant role in determining the strength. Once nucleated by slip, they may grow, increase in number density, or propagate rapidly if the tensile stress normal to the plane on which they lie is sufficiently high. In any case, the resistance of ice to crack propagation is a factor which must be considered when dealing with the forces exerted by ice on engineered structures.

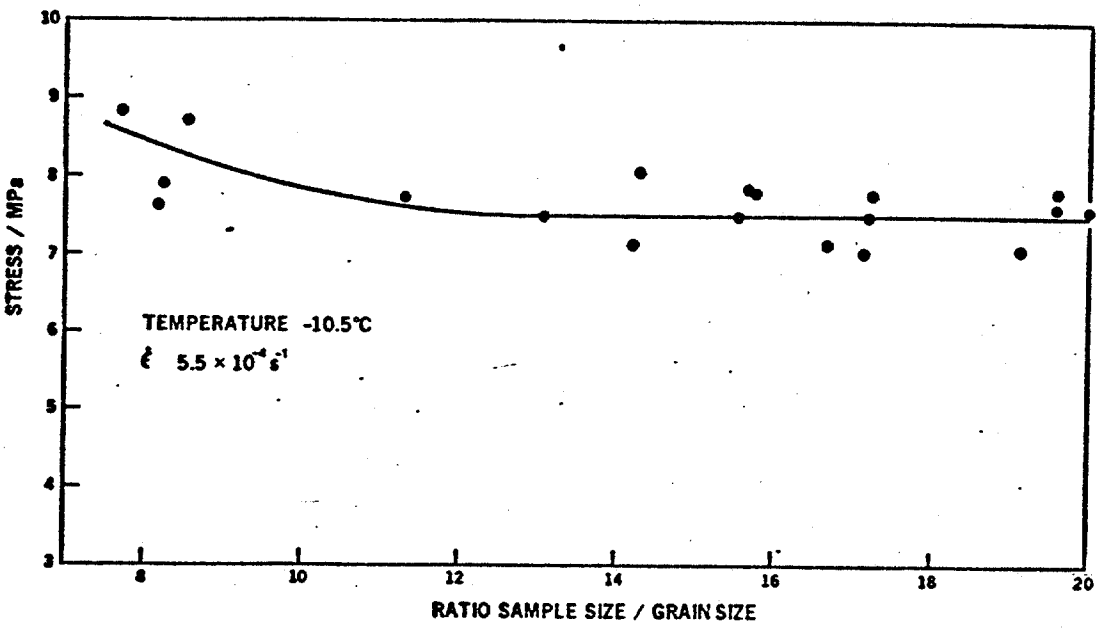

Figure 13. Plot of the peak stress (see Fig. 10) in compression versus the ratio of sample size to grain size. The grain size was held constant at 1 mm and the sample diameter varied. (Taken from reference 45)

In dealing with fast crack propagation -- i.e. propagation which is not accompanied by extensive plastic deformation -- linear elastic fracture mechanics is appropriate. In this case, the stress intensity factor, K, and the critical stress intensity factor, K_c, termed the fracture toughness, are of interest. When dealing with propagation which is accompanied by elastic and by plastic deformation, then a different approach is needed, one which incorporates the stress/strain conditions which exist near the tip of the crack within an elastic/plastic solid. In this case, the J-integral approach may be appropriate or a modified[55] J-integral approach which incorporates creep deformation. However, unlike linear elastic fracture mechanics, elastic/plastic mechanics is still in the developmental stages, and so the use of the concept in engineering design is not as immediate.

Incidentally, in the limit, the J-integral approach meets the K approach. J is regarded as the general fracture energy release rate. In the limit it is equivalent to $\mathcal{G}$, the elastic energy release rate for the purely elastic case; K and $\mathcal{G}$ are related by the expressions:

$$\left.\begin{aligned} K_c &= (E\mathcal{G})^{\frac{1}{2}} && \text{(plane stress)} \\ K_c &= \left(\frac{E\mathcal{G}}{1-\nu^2}\right)^{\frac{1}{2}} && \text{(plane strain)} \end{aligned}\right\} \quad [13]$$

where E is Young's Modulus and ν is Poisson's ratio.

From the viewpoint of ice mechanics, the tensile strength under rapid loading and the bend strength are probably determined by the plane strain fracture toughness, denoted K_{IC}. (The I denotes mode-I failure (versus II and III) where the crack surfaces move directly apart rather than sliding in-plane (mode II) or tearing anti-plane (mode III).) This parameter is to stress intensity what the yield strength, σ_y, is to stress: K_{IC} is the critical value of the stress intensity where cracks begin to propagate rapidly, just as the yield strength is a critical value of the applied stress at which

dislocations begin to slip. Like σ_y, K_{IC} is a materials parameter. In dealing with ice which is cracked prior to loading, then the K_{IC} approach is appropriate, provided that the tensile stresses are rapidly applied and that the ice is thick. This approach is routinely used when predicting the integrity of large welded structures which contain cracks within the welds.

Even under conditions for which its use is justified, linear elastic fracture mechanics appears not to have been accepted by workers concerned with ice. One reason appears to be the fact that K_{IC} decreases with increasing temperature, whereas the reverse happens in metals. This unusual characteristic was first noted a decade ago[56] and has since been verified by a fairly comprehensive study[29] of the fracture toughness of fresh-water ice, Figure 14. This effect may be caused by the formation of a liquid layer on the surface of ice, a transformation which is thermodynamically stable[57] and which lowers the surface energy: the higher the temperature, the thicker is this layer. Whatever its origin, the effect appears to be real and should be taken into account. It should not, however, stand in the way of seriously exploring what may turn out to be a useful method for predicting the strength of cracked or flawed ice.

How does one apply the K_{IC} concept, and what evidence is there that it can meaningfully predict the strength of sea ice, say? Concerning the first question we may write (following our earlier discussion on tensile strength):

$$K_{IC} = Y \sigma \sqrt{C} \qquad (14)$$

where σ is the maximum principal stress (tensile) acting on a body of ice, C is one-half of the crack length, and Y is a geometrical factor of order unity. The value of K_{IC} is set by the conditions (temperature, Figure 14, and structure, discussed below) of the ice and by the rate of deformation (also Figure 14). Thus, for ice containing cracks of a given size, the tensile strength may be estimated directly from equation (14).

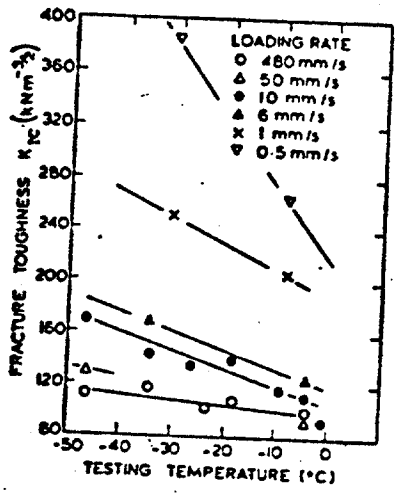

Figure 14. Fracture toughness, K_{IC}, of ice as a function of temperature for six different loading rates (taken from ref. 55 which was obtained from the data in ref. 29). Note that K_{IC} decreases with increasing loading rate.

Concerning the evidence, studies[57] of the plane strain fracture toughness and the bending strength, σ_b, of sea ice taken from an inland sea in Japan ("Lake" Saroma) indicate a good correlation between the value of the crack size deduced from equation (14), using $Y = \pi^{\frac{1}{2}}$,

$$C = \frac{1}{\pi}\left(\frac{K_{IC}}{\sigma_b}\right)^2 \quad , \tag{15}$$

and the size of the subgrains within the aggregate. Cracks were run both from the top (i.e. ice/air interface) and from the bottom (ice/water interface) surfaces of notched and of unnotched beams; i.e. they were started in regions having either a fine (top) or a coarse (bottom) microstructure. The average values of C calculated from equation (15) were 19 $\pm$ 5 mm and 2.5 $\pm$ 1 mm, for the bottom and top surfaces, respectively, versus grain diameters of 20 to 30 mm and 2 to 5 mm. This agreement suggests that, in sea ice, the "flaw" size correlates with the subgrain size. Once known, then the strength in tension and in bending may be predicted from the K_{IC} approach, again for thick ice rapidly loaded.

Not surprisingly, the measured values of K_{IC} for the above sea ice were dependent upon the scale of the microstructure through which the crack propagated. Cracks started at deep notches on the upper surface propagated through the coarser material near the bottom; alternatively, those started at notches on the lower surface propagated through the finer material near the top. Correspondingly, the fracture toughness associated with the coarse structure was lower than with the finer structure -- $\simeq$ 0.05 MPa$\cdot$m$^{\frac{1}{2}}$ versus 0.08 $\pm$ 0.01 MPa$\cdot$m$^{\frac{1}{2}}$. Nor is it surprising that the fracture toughness of columnar sea ice was found to be lower than that for columnar fresh-water ice, the latter being 0.11 $\pm$ 0.02 MPa$\cdot$m$^{\frac{1}{2}}$ at $-2°C$.[28,29] Needle-like brine cells of sea ice probably lead to stress intensification additional to that caused by a sawn and sharpened notch in a test block, and in the presence of sea water

at -2°C (which surrounded the test material[57]) grain boundaries may have become deeply etched, thereby acting as further stress concentrators. In other words, the effective crack size in the test blocks may have been deeper than appreciated, implying that the apparent toughness as measured may be lower than the real toughness.

In criticizing the K_{IC} measurements made to date, it could be said that insufficient attention has been paid to geometrical effects; i.e. to the ratio of specimen size to grain size, and to notch acuity. If too small, both could lead to apparent values larger than true values. Also, little attention has been paid to microstructure. Are fine-grained aggregates tougher than coarse-grained ones, as implied by the results on sea ice? Similarly, little attention has been given to possible environmental effects. Does brine lower K_{IC}? Attention to such details would assist the transfer of this kind of methodology from solid mechanics to the mechanics of sea ice and should be incorporated within testing programs.

To summarize, fracture mechanics should be applied to ice, but care must be taken in selecting the appropriate fracture toughness parameter. The plane strain fracture toughness, K_{IC}, the J-intregral and even a creep-modified J-integral approach are contenders. Which is the most suitable will depend upon the mass and size of the ice and on the rate and temperature of loading. It could be troublesome, for instance, to use K_{IC} to predict the force required to bend a sheet to fracture, given a crack of known depth in from the tensile surface, if the sheet were thin (relative to the size of the plastic zone at the top of the crack), if the ice were "warm", and if the load were slowly applied. The number obtained would not include plastic flow and the stress redistribution due to relaxation and would, therefore, be on the low side. In engineered structures, application of K_{IC} to situations in which the approach is not strictly justified leads, if anything, to a conservative

estimate of the stress which a flawed structure can bear, and this is useful. In ice mechanics, on the other hand, such estimates are of little value when the number of interest is the highest possible force which is needed to break the ice. In other words, fracture mechanics should be used in dealing with flawed ice, but used wisely.

10. CONCLUDING REMARKS

To summarize, ice Ih has been viewed within the context of materials science, with the goal of obtaining insight into its mechanical properties. Constitutive relationships previously published and based upon materials parameters have been discussed, and deformation mechanism maps, derived from such relationships, presented. Strength both in tension and in compression has been considered, and explanations have been generated which incorporate plastic flow both on "soft" and on "hard" slip systems plus crack nucleation and growth. The effects on strength of hydrostatic pressure and of general multiaxial loading (in the all-compressive octant) have been analyzed, and a "working hypothesis" invoking the idea of a critical shear stress presented for estimating strength under such conditions. Also considered are the possible/probable effects on strength of grain size, sample to grain size ratio and surface condition, the last point leading to a proposed criterion for the annealing out of possible machining damage. Finally, fracture mechanics has been discussed with emphasis on the role of this modern development in solid mechanics in predicting the strength of flawed ice.

A number of problems have arisen as a result of this study and are listed where appropriate in the text. Noticeable is the recurrence of questions concerning cracks. Once nucleated, do these features grow under a constant stress? If so, how quickly? Is there, as proposed, a critical crack number density necessary to trigger slip on "hard" systems? Is the ratio of the compressive strength (at high deformation rates) to the tensile strength equal to eight for pre-cracked ice containing relatively large and randomly oriented flaws? How ductile is ice when crack growth is suppressed by hydrostatic pressure or by general multiaxial loading? And does the average size of the largest grains (and hence crack), and not the average grain size, determine the strength of an uncracked polycrystal when loaded in tension? Related are questions regarding the appropriate fracture mechanics parameter which governs the strength of

thick and of thin flawed ice sheets loaded either rapidly or slowly in tension, and attendant questions concerning the effects of environment (e.g. brine), microstructural scale and specimen size on fracture toughness.

As noted in the Introduction, some of the comments and analyses and, hence, the questions arising are tentative. Hopefully, however, they will be of value in interpreting the results of test programs. Hopefully, too, they may help to chart further studies of this novel material.

REFERENCES

1. C.E. Bates, private communication, April 13, 1982; Southern Research Institute, Birmingham, Alabama

2. E. M. Schulson, Report on "The Velocity of Ultrasonic Waves Through Sea Ice Taken from Pressure Ridges Within the Beaufort Sea", April 26, 1982; submitted to E.N. Earle, May 3, 1982

3. Z. Hashin, J. Appl. Mech. 29 (1962) 143

4. J. K. MacKenzie, Proc. Phys. Soc. (London) 63B (1950) 2

5. R. L. Coble and W.D. Kingery, J. Amer. Ceram. Soc. 39 (1956) 377

6. "Constitutive Equations in Plasticity", ed. by A. Argon; The MIT Press, Cambridge, Mass (1975)

7. D.J. Goodman, H.J. Frost and M.F. Ashby, Phil. Mag. A 43 (1981) 665

8. S.J. Jones and J.W. Glen, Phil. Mag. 19 (1969) 13

9. H. Blicks, O. Dengel and N. Riehl, Phys. Conden. Mater. 4 (1964) 375

10. N.H. Fletcher, "The Chemical Physics of Ice", Cambridge University Press (1970)

11. M.F. Ashby, Acta Metall. 20 (1972) 887

12. H.J. Frost and M.F. Ashby, "Deformation Mechanism Maps"; Pergamon Press, Oxford, New York (1982)

13. M. Mellor and D.M. Cole, Cold Reg. Sci. & Tech. 5 (1982) 201

14. M.F. Ashby and N.J. Frost, Rept. CUED/C-MATS/TR26 (1976), Dept. of Engineering, University of Cambridge

15. L.J. Kuon and J.J. Jonas, "Physics and Chemistry of Ice", ed. by E. Whalley, S.J. Jones and L.W. Gold; Roy. Soc. of Canada (1973) 370

16. G.P. Rigsby, J. Glaciol. 3 (1958) 273

17. P.V. Hobbs, "Ice Physics"; Clarendon Press, Oxford (1974)

18. A.M. Brown and M.F. Ashby, Acta Metall. 28 (1980) 1085

19. L.W. Morland, Cold Reg. Sci. and Tech. 1 (1979) 101

20. L.W. Morland and U. Spring, ibid 4 (1981) 255

21. A.A. Griffith; Phil. Trans. Roy. Soc. (London) 221A (1920) 163

22. J.W. Hutchinson; Rep. MECH-1, Div. of Engineering & Applied Physics, Harvard U. (197

23. J.H. Currier and E.M. Schulson; Acta Metall. (in press)

24. D. R. Barker, M. Eng. Thesis, Thayer School of Engineering, Dartmouth College (June 1982)

25. J. R. Low, "The Relation of Microstructure to Brittle Fracture"; Trans. ASM 46A (1964) 162

26. G.W. Greenwood and A.G. Quarrell, J. Inst. Met. 82 (1954) 551

27. E.M. Schulson, Cold Reg. Sci. and Tech. 1 (1979) 87

28. D.J. Goodman and D. Tabor, J. Glaciol. 21 (1978) 651

29. H.W. Liu and K.J. Miller, J. Glaciol. 22 (1979) 135

30. A. Higashi, "Physics of Snow and Ice" (1967) 227

31. B. Michel, Can. Journal of Civil Eng. 5 (1978) 285

32. A.A. Griffith, "The Theory of Rupture", Proc. First Int. Conf. of Appl. Mech. (Delft) (1924) 55

33. F.A. McClintock and J.B. Walsch, Proc. Fourth U.S. Nat. Cong. Appl. Mech., Vol. 2 (1962) 1015

34. F.A. McClintock and A. Argon, "Mechanical Behavior of Materials", Addison & Wesley Publ. Co., Reading, Mass. (1966) 494

35. M. Mellor, "Physics and Mechanics of Ice", Ed. by T. Tryde, Springer-Verlag New York (1980) 217

36. I. Hawkes and M. Mellor, J. Glaciol. 11 (1972) 103

37. D.M. Cole and W. St.Lawrence, Proc. Third Conf. on Acoustical Emission/ Microscopic Activity in Geology, Structures and Materials (Oct. 1981), Penn. State (in press)

38. D. Carter, Doctoral Thesis, Dept. of Civil Eng., Laval University (May 1971)

39. C.J.L. Wilson and D.S. Russell-Head, J. Glaciol. 28 (1982) 145

40. S. Steinemann, Beitrage zur Geologie der Schweiz., Hydrologie 10 (1958) 1

41. J.J. Jonas and H.J. McQueen, "Treatise on Materials Science and Technology", Ed. by R.J. Arsenault, Vo. 6 (1975) 394

42. S.J. Jones, J. Glaciol. 28 (1982) 171

43. J.H. Currier, E.M. Schulson and W. St.Lawrence, Report USA-CRREL/Thayer School of Engineering (in press)

44. J. Muguruma, Brit. J. Appl. Phys. 2 (1969) 1517

45. S.J. Jones; to be presented at Second Symp. on Appl. Glaciology, CRREL, 23-27 August 1982; see also J. Glaciol. 27 (1981)1517

46. R.W. Baker, J. Glaciol 21 (1978) 485; also Science 322 (1981) 1043

47. P. Duval and H. LeGac, J. Glaciol. 25 (1980) 151

48. S.J. Jones, personal communication (June 1982); Fisheries and Environment Canada, Ottawa, Canada

49. J. Perry, personal communication (May 1975); Energy, Mines and Resources, Ottawa, Canada

50. B. Michel, "Ice Mechanics", Univ. of Laval Press, Quebec City (1978)

51. F. U. Hausler, Proc. IARH International Symp. on Ice, Laval University, Quebec City (1981), p. 389

52. A.G. Evans and R.W. Davidge, Phil. Mag. 20 (1969) 373

53. S.J. Schneider Jr. and R.W. Rice, ed., (The Science of Ceramic Machining and Surface Finishing", N.B.S. Special Publication 348, Washington, D.C. (1972)

54. R.O. Ramscier, J. Appl. Phys. 38 (1967) 2553

55. K.J. Miller, Proc. IUTAM (1979) p. 265

56. H.W. Liu and L.W. Loop, USA CRREL Technical Note (unpublished), February 1972

57. N. Urabe, T.Iwasaki and A. Yoshitake, Cold Reg. Sci. & Tech. 3 (1980) 29

APPENDIX 1

THE VELOCITY OF ULTRASONIC WAVES THROUGH SEA ICE TAKEN FROM PRESSURE RIDGES WITHIN THE BEAUFORT SEA

ERLAND M. SCHULSON

April 26, 1982

ABSTRACT

Experiments have revealed that the velocity of longitudinal ultrasonic waves (10^6 cps) through ice taken from pressure ridges within the Beaufort Sea is 3840 $\pm$ 120 m/sec at approximately -22°C, ostensibly independent of the depth beneath the surface from which the ice was taken. In view of this result and of the variability of the ice examined, it is probable that the velocity of sound will not correlate with the strength of this material.

1. INTRODUCTION

Ultrasonic inspection is a non-destructive method of detecting internal flaws within solids. Waves of high frequency (typically, 1 to 25 MHz) travel rapidly through material ($\simeq$ 6000 m/sec, steel; $\simeq$ 4000 m/sec, ice), attenuate, and reflect off interfaces. Either the wave velocity, the degree of attenuation, spectral analysis, or echoes may be used to reveal defects.

For several years, researchers at the Southern Research Institute have been using this method to characterize cast iron.(1) They find that wave velocity in the axial direction of cylindrical castings correlates rather well with the axial tensile strength. Specifically, as the axial velocity decreases, owing to increases in the ratio of the surface area of graphite to the volume of the metal, the strength decreases. The sensitivity is such that a two-fold decrease in velocity corresponds to about a four-fold decrease in strength.(1)

With this correlation in mind, the question arose: Does the velocity of sound through sea ice originating in pressure ridges correlate with the

strength of this material? Like cast iron, sea ice contains an array of defects ranging from spherically shaped features (bubbles and brine pockets) to flake-like features (cracks), all of which may affect the strength.

To answer this question, a small experimental study has been initiated. The work to date has dealt specifically with sonic velocities and is summarized here. Later work, proposed below, will measure the strength of the test pieces used here and will examine the microstructure of the same specimens. When completed, the work will afford a firm answer to the question.

2. EXPERIMENTAL

2.1 Material

Both naturally occurring sea ice and artificially grown fresh-water ice were examined, the latter as a reference. The sea ice had been collected in the form of cylindrical cores in April 1981 from pressure ridges within the Beaufort Sea, as part of the Shell/CRREL program on sea ice. From this source, specimens for the present study were selected to include what is anticipated to be a broad range of structures, ranging from low-density snow ice to higher density sea ice. Included, therefore, were two specimens from within 100 cm of the surface (expected to be granular snow ice), two from deeper (250 to 313 cm) within a ridge (denser and probably columnar grained), plus two from still deeper regions (360 to 400 cm) in which the salinity was the highest. Two of these specimens were right, solid cylinders, 10.7 cm in diameter and 25.4 cm in length. The other four, also solid cylinders of the same length, had slightly reduced gauge sections (10.2 cm diameter) and had fastened to both ends "synthane" end caps. (The caps, unfortunately, had to be removed prior to measuring axial velocity.) The table in the next section lists the specimens according to the Shell/CRREL designation and gives the densities and the salinities.

The fresh-water ice was grown in the laboratory from deionized and degassed water. The specimens also were right solid cylinders, but slightly smaller -- 9.1 cm in diameter and 23.1 cm in length. Two specimens were prepared, each of equiaxed and randomly oriented grains. One was comprised of fine grains, 1.0 mm in diameter;* the other, of coarse grains 5.9 mm in diameter.

2.2 Transportation

The measurements were performed April 13, 1982 at the Southern Research Institute, Birmingham, Alabama, through the gracious cooperation of Drs. Charles Bates, John Koenig and Dale van Wagoner. To facilitate transportation, the specimens were placed into separate plastic bags, packed with twelve cold packs ("X-Cold Bricks", Pelton Shepherd Inc.) into a "freezer pack" and protected with snow. The freezer pack is simply a polystyrene box ($\simeq$ 5.1 cm thick walls) contained within a cardboard shell. The entire package was placed for three days into a cold room at -30°C and then, just before shipping, "topped off" with 2.3 kg of dry ice. Once cooled, the package was held at temperatures around room temperature for a period of 56 hours (i.e. during the return trip from Hanover to Birmingham) without melting. In fact, the cold bricks, which melt at -12°C, were still solid after the trip.

2.3 Measurement of Velocity

The ice cylinders were immersed into a bath of "mineral spirits" which, through the use of dry ice, had been cooled to and maintained at -22 $\pm$ 1°C, Figure 1. (The actual temperature of the ice during examination, although not know with certainty, was between -30°C, the temperature at the start of the journey, and -12°C, the temperature at which the cold packs soften. The estimated temperature is around -22°C, which is close to the average of the extremes and

*The grain size corresponds to the average spacing between grain boundaries as seen on planar sections under polarized illumination.

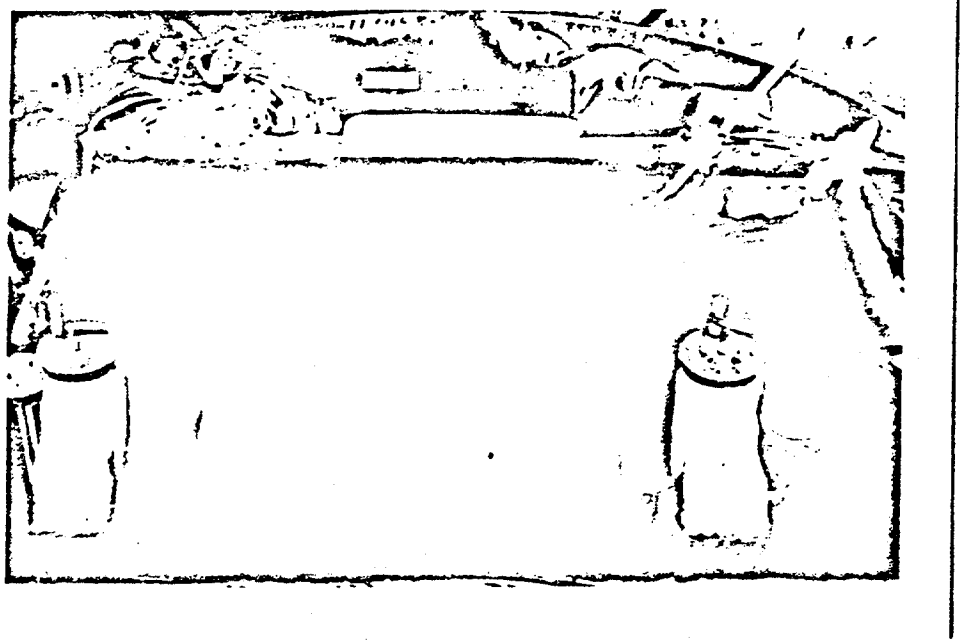

Figure 1. Photograph showing a specimen of sea ice immersed in a bath of mineral spirits. The transducers, which are located at but not attached to both ends of the cylinder, are just visible beneath the surface.

the same as the bath temperature.) The sonic frequency was 10^6 cps, and was selected on the basis of previous experience at the Southern Researhc Institute with coarse-grained materials. Prior to immersion, the length and diameter of the specimen were accurately measured, and the velocity of sound through the bath was experimentally determined for use in subsequent analysis. Sonic pulses were generated and detected using transducers made from $BaTiO_3$.

Velocities were measured across the diameter and along the length of the cylinders. The diametral velocities were obtained at ten positions, at five points along the axis for one orientation of the specimen and at five more points after rotating the specimen by 90° about its axis. Measurements of the axial velocities were made at five positions across one diametral chord.

All data were collected, stored and processed with the aid of Tektronix instrumentation, Figure 2. The author witnessed every test and Dale van Wagoner of Southern Research Institute directed every test, Figure 3.

3. RESULTS

The table lists the results plus the designation, the density, the salinity, and comments about the quality (visually determined) of each specimen. Owing to the constraints of time, only radial velocities were measured on the equiaxed and randomly oriented fresh-water ice, and only axial velocities were measured on three of the six specimens of sea ice. Unless tabulated, the deviation from the average measurement was less than 10 m/sec.

The results show that under the test conditions ($\simeq -22$°C; 10^6 cps) the velocity of longitudinal ultrasonic waves through ice is relatively insensitive to the source of the material. For instance, the difference between the velocity through equiaxed and randomly oriented aggregates of fresh-water ice (3918 m/sec; specimens 1 and 2) and that through lower density, high salinity sea ice (3997 m/sec; specimen 8) is less than 2% of the reference velocity.

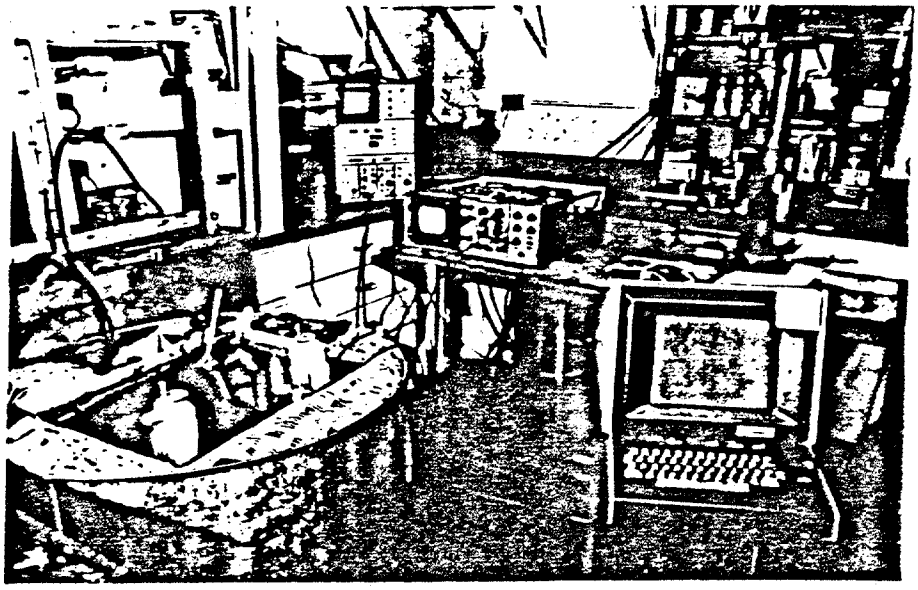

Figure 2. Photograph showing the equipment (Tektronix electronics) used in the measurements of ultrasonic velocity through ice

Figure 3. Photograph showing the author (foreground) and Dr. Dale van Wagoner witnessing a series of measurements on one specimen.

Velocity of Sound Through Sea Ice at Approximately -22°C

Specimen No.	Designation*	Density (g/cm^3)	Salinity (parts per thousand by weight)	Velocity (m/sec) Axial	Velocity (m/sec) Radial	Comments on Structure/ Quality of Ice
1	PL-41-fw	0.916	0	-	3918	d=1.0 mm**
2	PL-43-fw	0.916	0	-	3915	d=5.9 mm
3	R2A 45/72	0.825	0.28	3898	-	snow ice; void sheets
4	R2A 75/102	0.843	0.79	3504	3604 ± 20	
5	R1D 250/277	0.910	0.96/2.32	3830	4058 ± 32	grey ice
6	R1C 286/313	0.916	2.43	3910	4000 ± 40	grey ice
7	R1D 363/390	0.903	3.13	3884 ± 18	-	grey ice with breccia
8	R1D 392/419	0.886	3.13	3997	-	clear, white ice over half length; rest bubbly

*f.w. = fresh water ice.

The designation of sea ice is the one used in the Shell/CRREL program. For instance, R2A 45/72 means that the specimen was taken from site A within ridge 2 and that its top and bottom surfaces, respectively, correspond to depths of 45 and 72 cm.

**d = average grain size as described in Section 2.1

Over the complete range of material tested, the velocity varies by less than 500 m/sec; i.e. by ≈ 10%.

Ostensibly, the results as a whole also suggest that the sonic velocity in sea ice does not vary in any consistent manner with depth within the ridge. Rather, it seems that velocity is best expressed as an average of 3840 ± 120 m/sec. It is possible, however, that the velocity increases very slightly with depth once the superficial snow ice has been penetrated, judging from the results obtained from three samples taken from one site within one ridge (specimens 5, 6 and 8).

In the cases where both the axial and the radial velocities were measured, the latter are consistently about 3 to 4% higher than the former.

Generally, the degree to which the intensity of the ultrasonic wave decreased as it passed through the samples showed little variation from one specimen to another or from one position to another on a given specimen. However, in one case, specimen 4, the attenuation accompanying radial transmission varied by a factor of approximately 1.5. Figure 4 illustrates this point. The added attenuation in this case is attributed to the presence of sheets of voids which could be seen by the unaided eye to be aligned approximately in a radial direction. Extra reflections, presumably, occurred from the ice/void interfaces.

4. DISCUSSION

The result that the velocity of sound through ice is relatively insensitive to the origin of the material means that ultrasonic inspection, as utilized here, offers little scope as a method for quickly characterizing sea ice. Therefore, unlike the case with cast iron, it is highly probable, although not certain until mechanical testing and structural examinations have been performed, that the velocity of sound will not correlate with the strength of sea ice taken from pressure ridges.

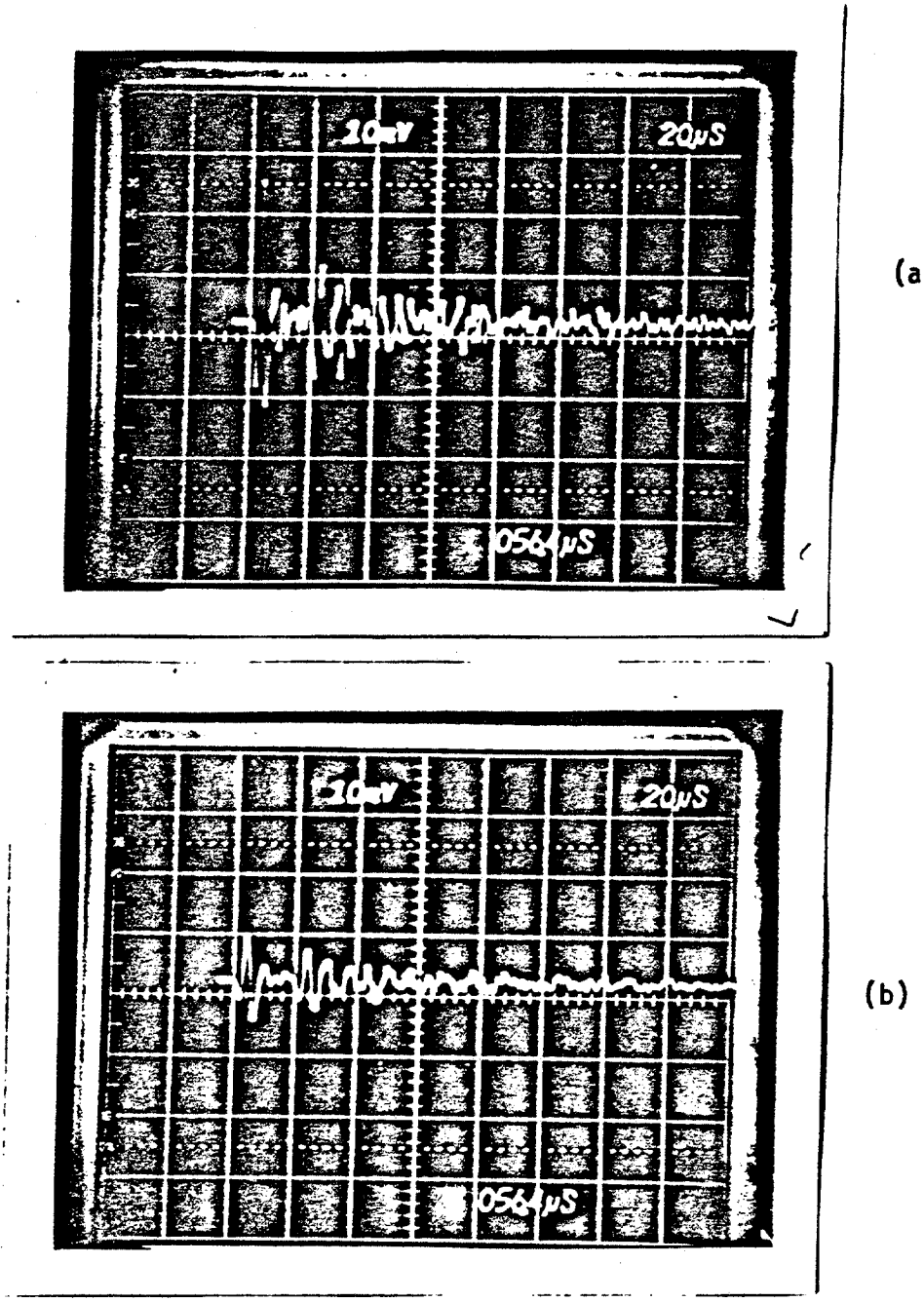

Figure 4. Photographs showing the attentuation in the amplitude of an ultrasonic wave as it traverses in a radial direction one specimen (No. 4 in table) at two separate locations along its axis. Note the greater degree of attenuation in (b), corresponding to propagation through a region containing sheets of voids radially aligned.

This is not to say that ultrasonic inspection in every form would be of no use in characterizing test material. Attenuation offers a potential tool, as does pulse - echo analysis. Both variations, however, would require extensive development incorporating standards having well characterized defects. Yet, even if these variations were developed, it is probable that, unlike the case with velocity, interpretation would not be unambiguous.

At this juncture, therefore, it appears that ultrasonic inspection holds little promise as a non-destructive method for rapidly characterizing ice.

It could be argued that this conclusion, particularly as it relates to ultrasonic velocity, is valid only for frequencies around 10^6 cps. Yet, higher frequency signals result in smaller wavelengths which may lead to extensive scattering in aggregates as coarsely structured as sea ice and, correspondingly, to invalid inspections. And lower frequency signals could possibly result in relaxation effects which could invalidate the results.

An implication of the results is that Young's modulus varies, given the variation in density and relative constancy of velocity.

4. CONCLUSIONS

1) The velocity of longitudinal ultrasonic waves (10^6 cps) through ice taken from pressure ridges within the Beaufort Sea and cooled to approximately -22°C is 3840 $\pm$ 120 m/sec.

2) The velocity appears to be independent of the depth beneath the surface from which the ice was taken.

3) Although uncertain, it is highly probable that the velocity of sound will not correlate with the strength of this material.

5. RECOMMENDATIONS

In the interests of completing the study, it is recommended that Shell authorize G. Cox of U.S.A. CRREL to bond end caps to two of the specimens and to re-bond end caps to the other four specimens to allow both mechanical testing under uniaxial compression at -20°C and at a strain rate of 10^{-3} sec^{-1} and structural examinations of deformed aggregates.

ACKNOWLEDGEMENTS

I would like to thank C.E. Bates, J. Koenig and D. van Wagoner, all of the Southern Research Institute, for kindly providing both time and facilities for carrying out the measurements in this report. Also, I acknowledge G. Cox and A. Bosworth of U.S.A. CRREL for providing and preparing the test specimens of sea ice, and P. Lim of the Thayer School of Engineering, Dartmouth College, for preparing the fresh-water ice.

REFERENCE

1. Charles E. Bates, Southern Research Institute, Birmingham, Alabama; private communication, April 13, 1982.

Appendix 2

COMMENTS ON THE ARRHENIUS DESCRIPTION OF DEFORMATION

From the discussion attending the constitutive relationships, we note that at all levels of stress the strain rate is expressed by an equation which contains an exponential function, $e^{-Q/kT}$, where Q is an apparent activation energy, T is temperature (absolute), and k is Boltzmann's constant. Although not explicit in the formulation for diffusional creep, the function is implicit, because diffusion coefficients, both for boundary and for volume (or lattice) transport, contain it. It has been suggested,[35] however, that such a description has no special merit as a mathematical description of thermal dependence on the basis that the significant properties of the function appear only at temperatures far above those at which ice exists.

Physically, $e^{-Q/kT}$ may be regarded as the probability that thermal energy (kT) provides to an atomic array a fluctuation in energy equal to or greater than Q. The higher is Q or the lower is T, the lower is the probability that this will happen. Consequently, at a given temperature, processes having a high activation energy have a lower probability of being activated than ones having a low Q. Similarly, a given process has a higher probability of being thermally activated the higher is the temperature. Thus, $e^{-Q/kT}$ has sound physical meaning because it has a firm basis in statistical mechanics.

To note that $e^{-Q/kT}$ has no significant properties at low temperatures is somewhat misleading. On a linear scale, it may appear to be doing nothing as temperature changes up to the melting point of ice. Yet on a semi-log scale the function rises rapidly with temperature, and it is this latter character which is so important.

Even though Q increases with temperature in polycrystals deformed above about -10°C, this is no reason to discredit the description, for in this range of temperature the dominant strain-producing mechanism is changing with temperature.

Thus, there is good physical reason for maintaining the exponential description of the variation in deformation rate with temperature.

Appendix 3

FLOW STRESS IN RELATION TO THE PRESSURE MELTING POINT

As hydrostatic pressure increases, the melting point of ice decreases, at the rate of 1°C per 10 MPa. As a result, ice which is held at one temperature -- say at -10°C -- is brought closer to its melting point. For instance, if the hydrostatic pressure is increased from atmospheric pressure to 50 MPa, then the homologous temperature of ice, held at -10°C, is increased from $\frac{263}{273} = 0.96$ to $\frac{263}{268} = 0.98$. Accordingly, the flow stress decreases when the rate of strain is held constant.

To account for this effect, it is suggested that the phenomenological constitutive equation (No. 5, p. 13) be written to include temperature, T, explicitly, and to include the hydrostatic component, σ_h, of the stress state. Thus, the shear strain rate, $\dot{\gamma}_S$, may then be written as:

$$\dot{\gamma}_S = B \sigma_S^n e^{-Q_{eff.}/kT} \qquad \text{(A3-1)}$$

where B and n are materials constants, σ_S is the equivalent shear stress, and k is Boltzmann's constant. $Q_{eff.}$ is the effective apparent activation energy for plastic flow and is scaled relative to the effective melting point. In other words, of the paramters united in equation A3-1, the activation energy is the one to display the effect of hydrostatic pressure. It does this via the expression:

$$Q_{eff.} = \left(\frac{T_{eff.}^{(m.p.)}}{T_o} \right) Q_o \qquad \text{(A3-2)}$$

where $T_{eff.}^{(m.p.)}$ is the effective melting point reflecting the hydrostatic pressure, T_o is the melting point at atmospheric pressure, and Q_o is the activation energy at atmospheric pressure. Hydrostatic stress is incorporated via the relationship:

$$T_{eff.}^{(m.p.)} = T_o - \lambda \sigma_h \qquad \text{(A3-3)}$$

where $\lambda = 0.1$ K/MPa. Here, σ_h is algebraically greater than zero for a compressive stress. Equation A3-1 may then be rewritten to incorporate hydrostatic pressure (i.e. σ_h) directly:

$$\dot{\gamma}_S = B \sigma_s^n \exp \{- \frac{Q_o}{kT} (1 - \frac{\lambda \sigma_h}{T_o})\} \qquad (A3\text{-}4)$$

The flow stress may then be obtained by rearranging equation A3-4.

This analysis suggests that if the hydrostatic pressure is increased from one atmosphere to 50 MPa, then the flow stress of ice at -10°C will decrease by about 20%, for a fixed rate of strain, assuming that Q_o = 0.8 ev/atom = 76.8 KJ/mole and that n = 3.

It is emphasized that this analysis is a phenomenological approach to the problem of accounting for the effects of hydrostatic pressure on the flow stress. A physical approach is more desired, but must await a more detailed understanding of the mechanism (vacancy-assisted? interstitial-assisted?) underlying plastic flow in ice very near to its melting point.

Appendix 4
GRAIN GROWTH IN ICE AT -10°C

Figure A4-1* shows a thin (≃ 0.5 mm) polycrystalline aggregate of fresh water ice, formed on a substrate of glass, which was held at -10°C for seven days. Figure A4-2 shows another aggregate, doped with NaCl (1.71×10^{-2} M NaCl initial solution), also held for seven days at -10°C. For comparison, this figure also shows the aggregates after holding for one-half houar at -10°C. There is little doubt that grain growth occurs under these conditions. In both cases, doped and undoped, the average grain diameter increased from around 0.15 mm to 1 mm within one week.

It could be argued that the phenomenon noted above is influenced by the high surface to volume ratio of the thin specimen; i.e. by the free surface. On the other hand, when cognizance is taken of the fact+ that the growth of fine grains (< 1 mm) in bulk ice at -10°C occurs at about the same rate as that in thin sections cut from the same piece of ice, then the suggestion on page 36 of the text that significant growth probably occurs in fine-grained bulk ice during storage at -10°C becomes meaningful.

---

*H.H.G. Jellinek and V.K. Gouda: Phys. Stat. Sol. 31 (1969) 413

+A. Gow, USA-CRREL, Hanover, N.H.: unpublished results (personal communication, May 1982)

Fig. 1. Pure ice, −10 °C, one half hour after preparation of specimen (65 ×)

1/2 hour

Fig. 3. Pure ice, −10 °C, seven days after preparation (25 ×)

7 days

Figure A4-1. Optical micrograph showing grains of ice within a thin polycrystalline aggregate held at -10°C for 1/2 hour and for 7 days (H.H.G. Jellinek & V.k. Gouda, Phys. Stat. Sol. 31 (1969) 413

Fig. 4. Doped ice (1.71×10^{2} M NaCl initial solution), −10 °C, one half-hour old (65 ×)

1/2 hour

Fig. 6. Doped ice, −10 °C, seven days old (25 ×)

7 days

Figure A4-1. Optical micrograph showing grains of ice within a thin polycrystalline aggregate, doped with NaCl, held at -10°C for 1/2 hour and for 7 days. (H.H.G. Jellinek & V.k. Gouda, Phys. Stat. Sol. 31 (1969) 413